ROBUST CONTROL OF A PNEUMATIC SYSTEM

by

Chutchpimuck Somboon

A Thesis Submitted in Partial Fulfillment of the Requirements for the Degree of
Master of Engineering in Mechatronics

Examination Committee: Prof. Manukid Parnichkun (Chairperson)
Dr. Mongkol Ekpanyapong
Dr. Tanujjal Bora

Nationality: Thai
Previous Degree: Bachelor of Engineering in Mechanical Engineering
Sirindhorn International Institute of Technology
Rangsit, Thailand

Scholarship Donor: Royal Thai Government Fellowship

Asian Institute of Technology
School of Engineering and Technology
Thailand
May 2021

AUTHOR'S DECLARATION

I, Chutchpimuck Somboon, declare that the research work carried out for this thesis was in accordance with the regulations of the Asian Institute of Technology. The work presented in it are my own and has been generated by me as the result of my own original research, and if external sources were used, such sources have been cited. It is original and has not been submitted to any other institution to obtain another degree or qualification. This is a true copy of the thesis, including final revisions.

Date: 10 May 2021

Name: Chutchpimuck Somboon

Signature:

ACKNOWLEDGMENTS

First, I would like to exhibit my virtuous respect to my advisor, Prof. Manukid Parnichkun, for his treasure guidance, suggestion, and encouragement in the overall study. Without his recommendations, it is impossible to finish this thesis.

I wish to extend my appreciation to Dr. Mongkol Ekpanyapong and Dr. Tanujjal Bora, the examination committees, for their valuable comments and knowledge sharing.

Moreover, I would like to extend my thanks to Mr. Hoang Hung Manh, the technical staff of the mechatronics department laboratory. He kindly offers me the resources in running the program.

I also would like to express my special thanks to the Royal Thai Government for providing financial support in my entire master's program in AIT.

Last, I wish to thank my parents for their support and assistance throughout my study.

ABSTRACT

In industrial applications, the PID controller has used because its structure is simple and easy to implement in the system. On the other hand, this controller still has an inevitable disadvantage which is it lacks robustness. As a consequence, the robust controller designed by the H-infinity technique is applying. Conventional H-infinity is a method to create a Robust controller by computing H-infinity controller γ -iteration. The loop-shifting two-Riccati formulae are solved to find the optimal γ so that the cost function satisfies under desired tolerance. This controller is a complex one due to the higher-order terms that make it is difficult to implement in the real system. However, it can provide good robust performance. The PID controller with a derivative first order is used to compare performance with the proposed controller designed by the conventional H-infinity method. Furthermore, the robustness test by varying the load mass and pressure of the system.

CONTENTS

LIST OF TABLES

LIST OF FIGURES

Figures **Page**

Figures **Page**

LIST OF ABBREVIATIONS

PID = Proportional Integral Derivative

SMC = Sliding Mode Control

EHA = Electrohydraulic Actuator

SVF = State-Variable Filters

GMPF = Generalized Poisson Moment Functions

SRIVC = Simplified Refined Method

RMSE = Root Mean Square Error

CHAPTER 1
INTRODUCTION

1.1 Background

The pneumatic actuator, which uses compressed air to control and transmit energy, is one of the most widely used systems of industrial and non-industrial applications. It has been applying for several applications such as clamping, drilling, or sawing of industrial applications. Moreover, it consists of some advantages over hydraulic and electrical actuators. Besides, it has benefits of low component cost, high power-to-weight ratio, lightweight, and readily usable power source, etc. The working fluid of the system is compressible. As a result, the pneumatic actuator has high nonlinearities. According to the nonlinear characteristic of the pneumatic actuator, position control is hard to perform. The nonlinearities occur from several causes such as valve behavior, friction, and air compressibility. Finally, many techniques had developed to achieve a good performance.

In the present day, according to the simplicity and ease of implementation of the PID controller, this classical controller has developed several techniques to apply with the nonlinear system. The PI and PID controllers with the pneumatic actuator were studied in Design and experimental evaluation of a position controller for a pneumatic actuator with friction and A practical control strategy for servo-pneumatic actuator systems in 2005 and 1999, respectively. The resulting control of a modified PID controller improved the stability of the pneumatic actuator. Moreover, the modified PID had a simple structure which was a feature of using this type of controller. However, PI and PID controllers still provide poor control performance and low robustness due to some uncertainties. As a result, robust control approach proposes to design a controller that can handle uncertainty.

The Robust control purpose is to accomplish robust performance and stability within the bounds of the modeling error. In the late 1970s, Sliding Mode Control (SMC) was proposed to handle nonlinear systems. The SMC is one of the robust control techniques that insensitive to uncertainties of the system. In addition, it is used when the system requires robustness and the tracking error to be in the desired boundary. The successful studies of applying the SMC to the pneumatic system have shown in P. Korondi, J.

Gyeviki study in 2006 and J Song, Y Ishida in 1997. However, this method still has a major problem which is chattering. It is phenomenal that has a finite frequency and amplitude oscillation. As a result, the system has low control accuracy.

In the early 1980s, George Zames, J. William Helton, and Allen Tannenbaum introduced H-infinity methods to design robust controllers. Several techniques of H-infinity have been proposing to simplify the complexity of H-infinity. For example, H-infinity loop shaping combines the classical control method with H-infinity optimization. The H-infinity control addresses the stability and sensitivity in the calculation, but it requires high-level mathematical understanding. The H-infinity comes from the optimization of the infinity norm. Thus, it computes the optimal value of the H-infinity controller by solving two Riccati equations. The resulting output can achieve under the desired tolerance. Some studies represented the result of applying H-infinity to the unstable system.

In system identification of the pneumatic actuator, the linear dynamic model of the position output of the actuator to input voltage applying to the valve is derived from the mathematic equations. The resulting model is described as a third-order dynamic system. Moreover, the model consists of a pole at an origin point. The unknown parameters of the equation can be determined in various ways. Some papers directly measured the unknown parameters to identify the mathematical model, while others modified the plant with a proportional controller. The modified plant is expressed as a first-order time-delay model. However, the time delay of this modified plant is enormous. Thus, the model is suggested to approximate as a second-order time delay instead. It is said that the correctness of the second-order approximation is higher than the first-order approximation of the modified plant.

1.2 Statement of the Problem

Due to the nonlinearities from the compressed air, valve behavior, and friction the position control of the pneumatic system is difficult to perform. The uncertainties and disturbance are the causes that make the dynamic model of the pneumatic actuator is complicated to estimate. The position of the pneumatic actuator is controlled by the robust controller.

1.3 Objective

This thesis proposes a robust controller by H-infinity method to control the position of the pneumatic actuator. Then, compare its performance with the PID controller based on pole placement tuning method.

1.4 Limitations and Scope

1. A linear pneumatic actuator is used Cylinder's specification

Actuation:	Double acting
Maximum working pressure:	7 Bar
Degree of freedom:	1 Degree of freedom
Stroke length:	0.5 meters
Maximum load:	1.22 kg.

2. The robustness performance will be tested by varying load mass and air pressure.

CHAPTER 2
LITERATURE REVIREW

2.1 Open Loop Control System

A non-feedback system is known as an open-loop system. The input signal of this continuous control system is independent of the output. In other words, the desired output is accomplished without using the feedback. **Figure 2.1** depicts the open-loop control system black diagram.

Figure 2.1

The Open-Loop Control System Block Diagram

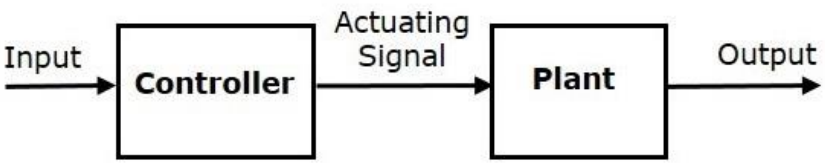

2.2 Closed-loop Control System

The closed-loop control system is a continuous control system that the input depends on the feedback output. In other words, the desired output of the closed-loop system is automatically provided to compare with the actual input. A block diagram of a negative feedback closed-loop control system is illustrated in **Figure 2.2**.

Figure 2.2

The Closed-Loop Control System Block Diagram

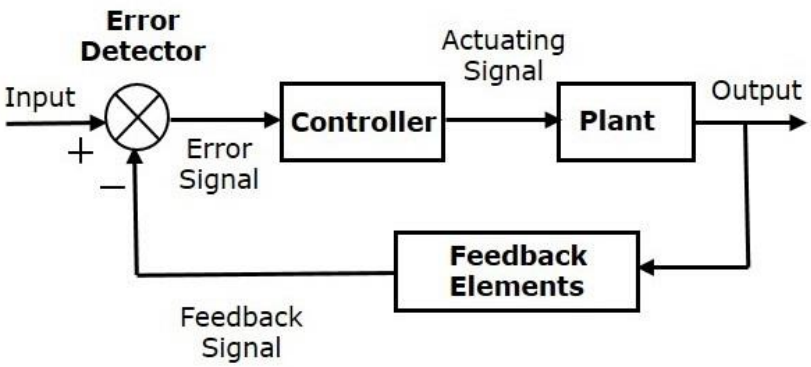

2.3 PID Controller

A proportional–integral–derivative controller (PID controller) is a control loop tool employing feedback that is the most common control algorithm used in several industrial and non-industrial applications. The error between the desired output and the actual output is calculated in every loop to compute for the improved control signal based on the proportional, integral, and derivative terms. Each term provides different benefits for the system.

2.3.1 Proportional Control

Proportional control is the term that describes the algorithm in which the control signal is proportionally dependent on the error.

$$F(s) = K_P E(s) \tag{2.1}$$

Where, F(s) is the divergence in the control signal and K_p is the proportional gain.

Figure 2.3

Proportional Controller with the Closed-Loop System

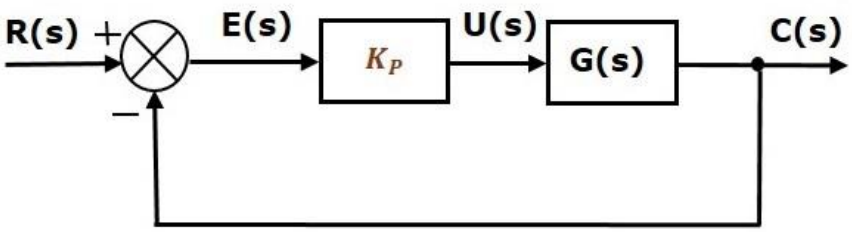

A first-order system when the step functions are applied as inputs,

1. Even there is no disturbance applied to the system, the output never reaches its final value. This error is called an offset error.
2. The time that it takes to approach the final value without oscillation, is inverse proportional to the proportional controller gain.
3. The inverse of the proportional gain equal to the output error from the disturbance at a steady state.

2.3.2 Integral Control

The offset error that happens from the proportional control can be developed by the integral control algorithm.

$$F(s) = \frac{K_I}{s} E(s) \quad (2.2)$$

$$f(t) = K_I \int_0^t e(t)\, dt \quad (2.3)$$

Where, K_I is the integral gain.

Figure 2.4

Integral Controller with the Closed-Loop System

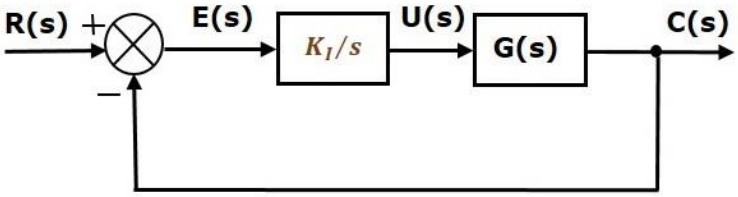

2.3.3 Derivative Control

Derivative control is applied to damp out oscillations. The derivative controller is the occasion of the derivative of the error signal.

$$F(s) = K_D s\, E(s) \quad (2.4)$$

$$f(t) = K_D \frac{d}{dt} e(t) \quad (2.5)$$

Where, K_D is the derivative gain.

Because of the error rate, derivative control must never be used alone.

Figure 2.5

Derivative Controller with the Closed-Loop System

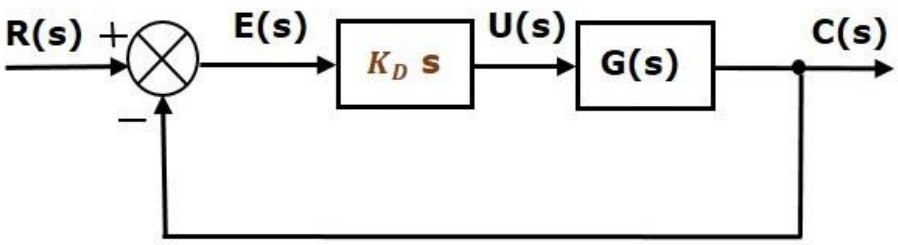

2.3.4 PID Control

The union of the proportional, integral, and derivative controller provides the output of the PID controller.

$$F(s) = \left(K_p + \frac{K_I}{s} + K_D s\right) E(s) \tag{2.6}$$

Figure 2.6

PID Controller with the Closed-Loop System

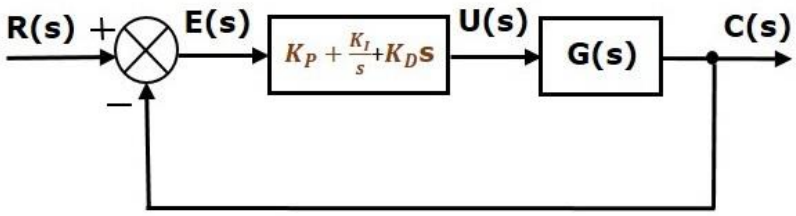

2.3.5 Advantages of the PID Controller

1. It does not require several sensors. In other words, it only acts on the error between the desired and the controlled signal. Therefore, extra measurements of the internal states are not necessary.
2. The tuning can be done easily by trial and error.
3. It is efficient and robust against some uncertainties if the system is properly tuned.
4. Inexpensive

2.3.6 Disadvantages of the PID Controller

1. The controller is not suited for nonlinear plants.
2. Derivative amplify noise

2.4 State-Space Control Theory

This part describes the state-space which is the classical control method. There are four approaches to the state-space. First, the first-order equations are used for all differential equations. Second, the number of the first-order equations defines the order of the system. Third, the state variables are the dynamic variables that represent in the first-order equations. Last, even though the identity of the state variables may not be unique, the number of these variables is unique.

For k order system, the state variables and control inputs can be expressed as:

$$x = \begin{bmatrix} x_1 \\ \vdots \\ x_k \end{bmatrix} \quad and \quad u = \begin{bmatrix} u_1 \\ \vdots \\ u_l \end{bmatrix} \tag{2.7}$$

Where, x = state vector and u = input vector.

In a linear process, the state equation can be shown as:

$$\dot{x} = A(t)x + B(t)u \tag{2.8}$$

$$A(t) = \begin{bmatrix} \mathrm{a_{11}(t)} & \cdots & \mathrm{a_{1k}(t)} \\ \vdots & \ddots & \vdots \\ \mathrm{a_{k1}(t)} & \cdots & \mathrm{a_{kk}(t)} \end{bmatrix} \text{ and } B(t) = \begin{bmatrix} \mathrm{b_{11}(t)} & \cdots & \mathrm{b_{1l}(t)} \\ \vdots & \ddots & \vdots \\ \mathrm{b_{k1}(t)} & \cdots & \mathrm{b_{kl}(t)} \end{bmatrix} \tag{2.9}$$

Where, A(t) = state matrix and B(t) = input matrix

For linear time-invariant processes, the state equation

$$\dot{x} = Ax + Bu \tag{2.10}$$

Where, A and B are constant matrices.

Measured outputs can be shown as:

$$y = \begin{bmatrix} y_1(t) \\ y_2(t) \\ \vdots \\ y_m(t) \end{bmatrix} \tag{2.11}$$

Where, y(t) = output vector or observation vector.

In a linear system the output vector can be expressed as:

$$y(t) = C(t)x(t) + D(t)u(t) \tag{2.12}$$

Where, C(t) = output matrix

For time-invariant, C(t) and D(t) are constant matrices.

$$y = Cx + Du \tag{2.13}$$

Furthermore, there are two types of input. The first one is the control inputs (u). They are produced intentionally by the operation of the control system. On the other hand, exogenous inputs are the second one. It shows in the environment and not subject to control within the system.

As a result, the general representation of a linear system is

$$\dot{x} = Ax + Bu + Ex_0 \tag{2.14}$$

A block diagram representing the general linear system is illustrated in **Figure 2.7.**

Figure 2.7

General Linear System Block Diagram

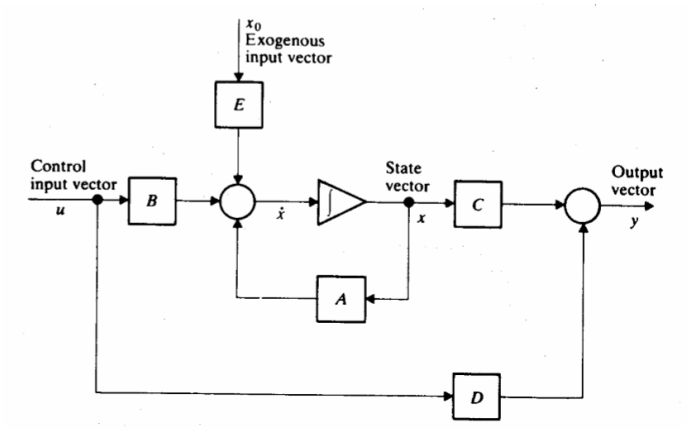

2.5 Robust Control

The controller that can deal with uncertainty is the one designed by a robust control method. Several techniques have been developed such as H-infinity loop shaping or sliding mode control. A block diagram of the Plant and Controller with disturbance input and disturbance output is illustrated in **Figure 2.8.**

Figure 2.8

The Plant and Controller Block Diagram with Disturbance Input and Reference Output

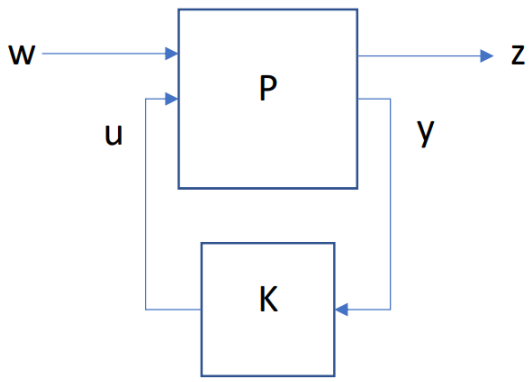

The open-loop system obtains from the above figure is:

$$\begin{bmatrix} z \\ y \end{bmatrix} = P \begin{bmatrix} w \\ u \end{bmatrix} = \begin{bmatrix} P_{zw} & P_{zu} \\ P_{yw} & P_{yu} \end{bmatrix} \begin{bmatrix} w \\ u \end{bmatrix} \quad (2.15)$$

While the closed-loop transfer function from disturbance as an input to reference as an output is:

$$T_{zw} = P_{zw} + P_{zu}K\left(I - P_{yu}K\right)^{-1}P_{yw} \quad (2.16)$$

2.6 H-infinity Loop Shaping

H-infinity loop shaping is one of the robust control techniques which is developed to deal with uncertainty. The sensitivity of the system controlled by this method is minimized for every value of frequencies, and the system deviation is guaranteed to be in the exacted trajectories even there are disturbances applied to the system. One of the most applied structures is PID with a filter derivative. The gains of the structure specified mixed sensitivity H_∞ controller obtained by using some optimization methods such as GA, PSO. The gain can be written as:

$$G = K_P + \frac{K_I}{s} + \frac{K_D s}{T_D s + 1} \quad (2.17)$$

In 2004, the research named a genetic algorithm-based fixed structure robust H_∞ loop-shaping control of a pneumatic servo system was conducted by Somyot Kaitwanidvilai. The robust controller was designed by optimal H_∞ control. The H_∞ loop shaping was implemented. In addition, The H-infinity loop shaping is optimized by the genetic algorithm. The performance of the PI, PID and the proposed H-infinity loop-shaping controller to control the pneumatic actuator is compared. The experiment was set up as shown in **Figure 2.9**. The experiment is tested by a pneumatic actuator with a stroke length of 200 mm, and it can work with a maximum pressure of 7 bars (0.7 MPa). The 5/3-ways proportional valve used in the test. A linear potentiometer was used to measure the position. The nominal pressure of 550 kPa is sustained by a pressure regulator.

Figure 2.9

Experimental Set Up of a Pneumatic Servosystem

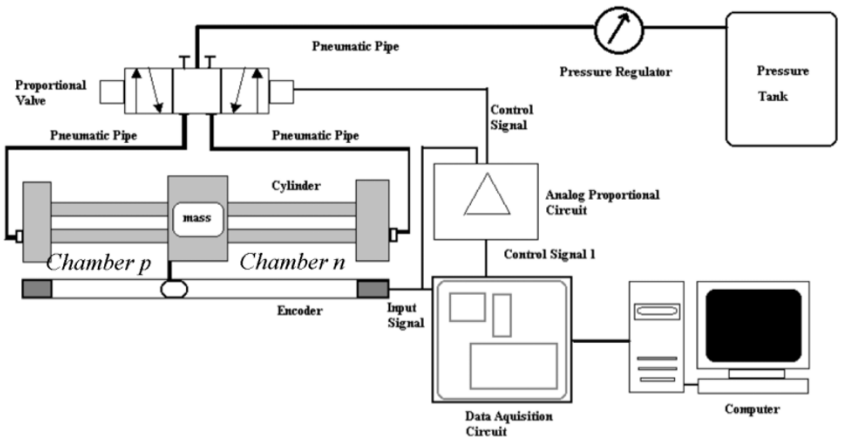

H_∞ loop-shaping control is an effective way to design a robust controller. The desired open-loop shape is required in this method. The weighting functions of W_1 and W_2 are used to shape the plant model to achieve the desired loop shape. The augmented plant is represented as G_s, and it is separated into the nominator N_s and denominator M_s factors. According to this approach, the shaped plant G_s can be expressed as:

$$G_s = W_2 G W_1 \rightarrow \begin{bmatrix} A & B \\ C & D \end{bmatrix} \tag{2.18}$$

$$G_s = (N_s + \Delta_{N_s})(M_s + \Delta_{M_s})^{-1} \tag{2.19}$$

The weighting function can be written as:

$$W_1 = K_W \frac{s+\alpha}{s+\delta}, \qquad W_2 = I \tag{2.20}$$

Where, K_W, α and δ are positive numbers.

Next, calculate the optimal cost which is the inverse of ε. The robustness of the desired loop shape is measured. After succeeding in the calculation for the, select the value of ε which is lower than the optimal one. Then, we will get the final K value of the controller as:

$$K = W_1 K_\infty W_2 \tag{2.21}$$

After obtaining the final value of the controller, the PID controller fixed-structured with a derivative first-order is applied. The structure of the controller is explained as:

$$K(p) = K_P + \frac{K_I}{s} + \frac{K_D s}{\tau_D s + 1} \tag{2.22}$$

K_P, K_I, K_D and τ_D are unknown parameters to be estimated.

Figure 2.10 illustrates the desired loop shape provided by the H_∞ controller. It explains that the proposed method can perform as a robust controller correlates to the desired loop shape. The bode plot of the PI and PID controller performs like the desired loop shape. The calculated value of the optimal stability margin ε_{opt} was founded to be 0.5793. Thus, for designing the robust controller, the ε is selected equal to 0.5475. After 100 generations of the genetic algorithm were run, the stability margin was 0.5298 and 0.4975 for the PID controller and PI controller, respectively. **Figure 2.11** represents a plot of the infinity norm of the cost function which is the inverse of the stability margin to each iteration of the genetic algorithm. According to the result of the ε, robustness can be guaranteed by the proposed robust controllers.

Figure 2.10

Bode Plot of Desired Loop Shape and the Proposed Controllers

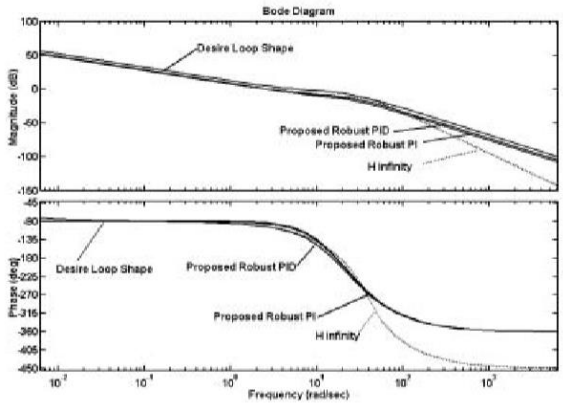

Figure 2.11

The Plot between Genetic Algorithm Iterations and the Cost Function

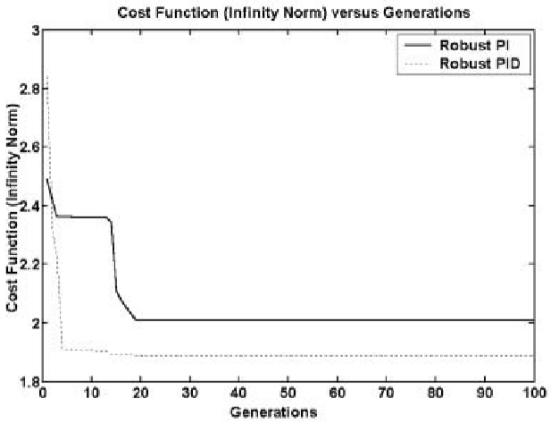

2.7 Sliding Mode Control (SMC)

Sliding mode control (SMC) is a powerful technique for robust control of nonlinear systems. The dynamics of a nonlinear system are changed by sliding along the surface.

In 2014, Xiaotao Liu et al., the sliding mode control was implemented to an electrohydraulic actuator (EHA) system. Normally, the hydraulic system is controlled by a valve. On the other hand, this paper proposed the EHA system controlled by a pump. The pump always provides the uncertainties, disturbances, and measurement noise to the system. Thus, the integral sliding mode control is suggested to control the system. The optimal feedback gain is derived by the H-infinity and the pole placement tuning method. The important and sufficient condition is calculated to obtain the optimal value. The sliding mode reaching law is satisfied by developing a sliding mode control law. To compare the performance of the proposed controller, the H_∞ PI plus feedforward controller was used as a comparison. **Figure 2.12** shows comparison of the performance between the proposed controller and the optimal H_∞ PI plus feedforward controller.

Figure 2.12

Comparison of the Control Performance between the Proposed Controller and the Optimal H_∞ PI Controller

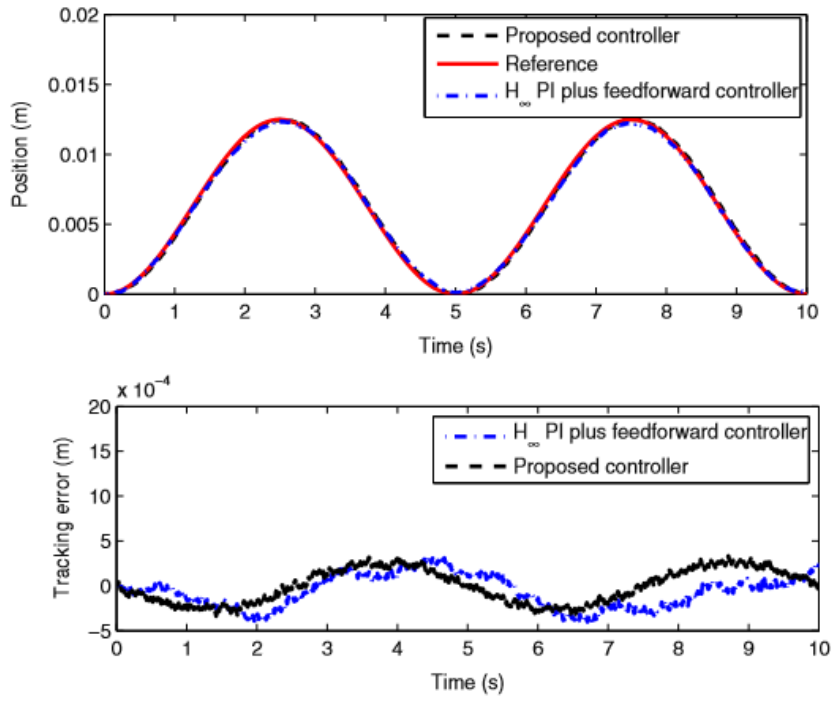

When the input to these two controllers was compared, the control input of the optimal H_∞ PI controller was approximately 5 times higher than the proposed controller. Because the optimal H∞ PI plus feedforward controller is sensitive to noise, the control input is extremely fluctuating when the uncertainty, disturbance, and measurement noise are applied to the system. In other words, it can be implied that the energy consumed by the optimal H∞ PI plus feedforward is greater than the proposed controller for a similar performance. **Figure 2.13** illustrates the control input to the proposed controller and the optimal H_∞ PI controller. Furthermore, **Figure 2.14** depicts that the proposed controller performs a much better tracking error than the optimal controller.

Figure 2.13

Comparison of the Control Input between the Proposed Controller and the H_∞ PI Plus Feedforward Controller

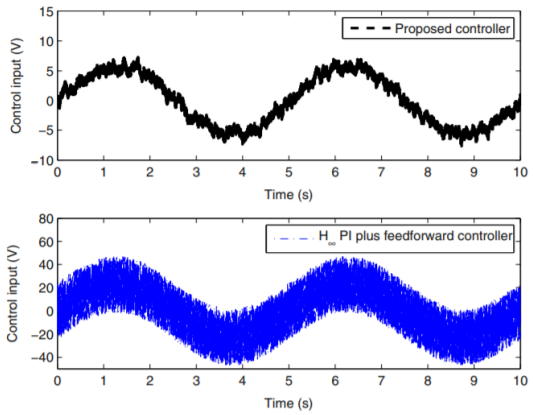

Figure 2.14

Control Performance of an Immediate Desired Position

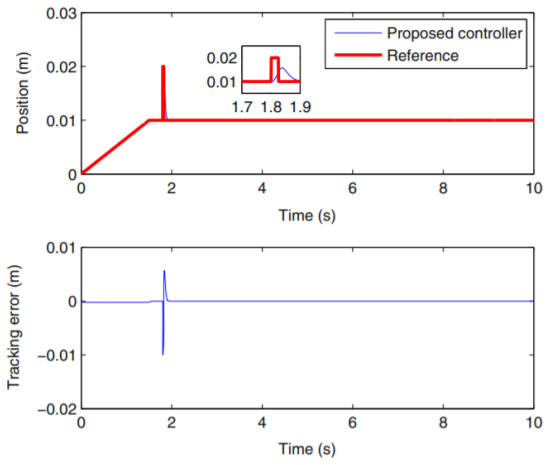

In conclusion, the sliding mode control is tested with the EHA system by proposing an integral sliding mode surface. The quasi-sliding mode surface can be reached by developed a sliding mode control law to drive the EHA system. The proof that the controller is robust to the acceptable bounded uncertainty is the value of the resulting stability margin.

2.8 H-Infinity Synthesis

H-infinity control, proposed by George Zames, J. William Helton, and Allen Tannenbaum is a method to design a robust controller which well handles uncertainties. The robust controller designed with this technique does not go unstable easily when faces with some disturbance or noise. The H-infinity synthesis is a powerful tool for designing robust multi-input/multi-output control system that the singular value satisfies the loop shaping specifications. The H-infinity optimal control computes continuous H-infinity for γ-iteration by solving two Riccati equations. The output γ is the optimal value which provides the acceptable cost function of the equation (2.23) under a preset tolerance.

$$\|T_{zw}\|_{\infty} \leq 1 \tag{2.23}$$

Where

$$T_{zw} \overset{\text{def}}{=} \begin{bmatrix} W_1 S \\ W_2 T \end{bmatrix} \tag{2.24}$$

The usual H-infinity control is sometimes referred to H-infinity small gain problem. Normally, the H_2 and H_∞ are simultaneously applied, the H_2 to perform the first cut to determine what level of performance can be achieved. Then, the outcome of the first process is used to select the H_∞ performance criterion. The H-infinity theory needs four necessary conditions.

1. D_{11} must be small enough to have constant feedback such that the closed-loop matrix satisfies.
2. The H-infinity full-state feedback control Riccati equation must have a real, positive semidefinite solution P.
3. The Riccati equation associated with observer dual of the H-infinity full-state feedback problem must have a real, positive semidefinite solution S.
4. The maximum eigenvalue of the resulting output of the two Riccati equations must be less than one.

It is necessary that these four conditions must be achieved to provide a feedback control law that the standard H-infinity control problem is solved. The search for optimal γ stopped when the γ relative adjacent error is less than the indicated limit.

Figure 2.15

Block Diagram of Controlled System with Disturbance

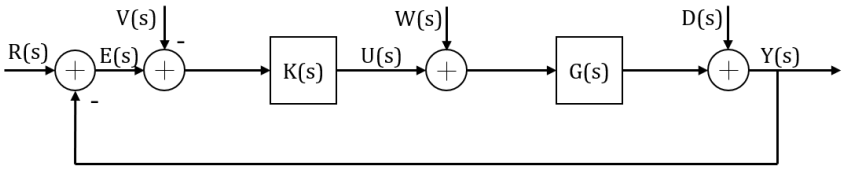

Figure 2.15 illustrates the block diagram of the system with disturbance where the plant is G(s), controller is K(s), with unity negative feedback. Disturbance input is in the form of reference input R(s), measurement error is V(s), actuator error is W(s), and output disturbance is D(s). According to the block diagram, the looping function is found as:

$$L(s) = G(s)K(s) \tag{2.25}$$

Sensitivity function is expressed as:

$$S(s) = \big(1 + L(s)\big)^{-1} \tag{2.26}$$

Complementary sensitivity function is:

$$T(s) = \big(1 + L(s)\big)^{-1} L(s) \tag{2.27}$$

Thus,

$$S(s) + T(s) = I \tag{2.28}$$

To design the controller such that provides the least influence of disturbance D(s) to output Y(s), and measurement noise V(s) to output Y(s),

$$min \left\| \begin{bmatrix} W_1 S \\ W_2 T \end{bmatrix} \right\|_\infty \tag{2.29}$$

Figure 2.16

Block Diagram of System Showing Influence of Measurement Noise to Output

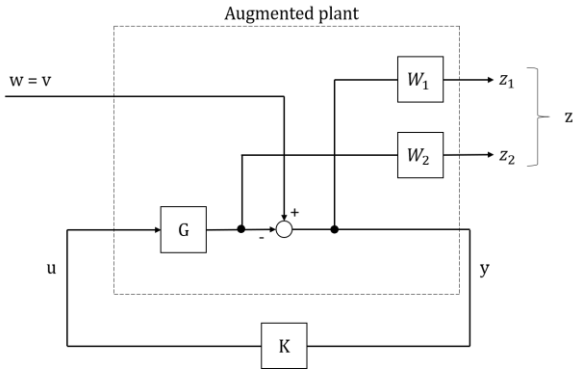

The augmented plant is expressed as:

$$P(s) = \left[\begin{array}{c|c} W_1 & -W_1 G \\ 0 & W_2 G \\ \hline I & -G \end{array}\right] \tag{2.30}$$

With state-space realization, it can be presented as:

$$P(s) = \left[\begin{array}{cc|c} A & B_1 & B_2 \\ C_1 & D_{11} & D_{12} \\ \hline C_2 & D_{21} & D_{22} \end{array}\right] \tag{2.31}$$

It is essential that the weighting functions are selected so that the generalized plant has a full column rank of matrix D_{12} or D_{12} must be a nonzero small value.

2.9 Weighting Function

The weighting function can be selected at any value depends on the task of the designed controller. Normally, W_1 is chosen large within the control bandwidth to get a small sensitivity function that provides good performance on reference tracking and disturbance rejection. W_2 is chosen large outside the control bandwidth to obtain small T for robustness and noise attenuation purposes.

In 2011, the automatic weight selection algorithm which used for designing an H-infinity controller was proposed by S. Nair. Weighting functions for designing an H-infinity controller conducted by a proposed algorithm called automatic weight selection. This algorithm provides the weight of W_1 and W_2 which the resulting cost function γ from the optimization process is lower than 1. The major disadvantage of this algorithm is that many parameters are needed to be fixed. Initially, the weighting functions are expressed as shown in equations (2.32) and (2.33).

W_1 or the weight function for sensitivity function, S(s)

$$W_1 = \frac{\frac{s}{M} + \omega_b}{s + \omega_b A} \tag{2.32}$$

where ω_b is the cut off frequency, M is the high frequency gain and A is the low frequency gain.

W_2 or the weigh function for complementary sensitivity function, T(s),

$$W_2 = \frac{Ls+1}{2(0.5Ls+1)} \tag{2.33}$$

where L is a constant.

Initially, this paper proposed that the starting value of A, M, and L is 0.1, 1, and 0.01, consecutively. The final value of A, M, and L for the weighting functions is accepted when the system meets all requirements shown in **Figure 2.17**.

Figure 2.17

Automatic Weight Selection Algorithm

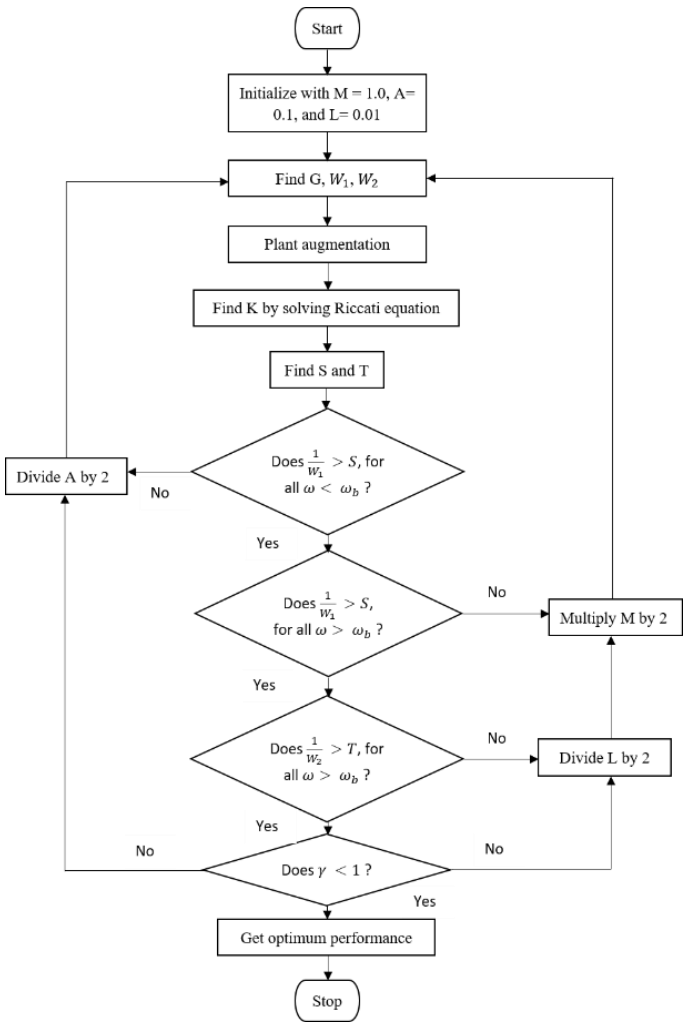

The resulting weight functions from the algorithm are shown in equation (2.34) and (2.35)

$$W_1(s) = \frac{0.33333(s+300)}{(s+5)} \tag{2.34}$$

$$W_2(s) = \frac{(s+100)}{(s++200)} \tag{2.35}$$

With the cost function γ equal to 0.7772.

To summarize, an automatic weight selection was proposed for synthesizing a robust H-infinity controller for active magnetic bearing systems. Two weighting functions normally came from the trial-and-error method. The H-infinity controller can be integrated from these weighting functions automatically. All requirements for designing an H-infinity controller have been made for this system.

2.10 Bilinear Transform

There are several methods to discretize continuous time-domain into discrete time-domain. Bilinear transform or Tustin's method is one of the discretization techniques used to transform a continuous-time system into a discrete-time. There are several methods to approximate the value on the z-plane from the s-plane. The first method is a first-order approximation.

$$z = e^{sT} \tag{2.36}$$

Need to linearize with Taylor series expansion:

$$z = e^{sT} = 1 + \frac{sT}{1} + \frac{(sT)^2}{2} + \frac{(sT)^3}{6} + \ldots \tag{2.37}$$

The higher-order term can be neglected because the value is very small. Thus, z can be written as:

$$z \approx 1 + sT \tag{2.38}$$

To put z in the form of $\frac{\text{a+bs}}{\text{c+ds}}$

$$e^{sT} = e^{\left(\frac{sT}{2}\right)}e^{\left(\frac{sT}{2}\right)} = \frac{e^{\left(\frac{sT}{2}\right)}}{e^{-\frac{sT}{2}}} \tag{2.39}$$

$$\frac{e^{\left(\frac{sT}{2}\right)}}{e^{-\frac{sT}{2}}} = \frac{1+\frac{sT}{2}+\frac{(sT)^2}{8}+\ldots}{1-\frac{sT}{2}+\frac{(sT)^2}{8}-\ldots} \tag{2.40}$$

$$z \approx \frac{1+\frac{sT}{2}}{1-\frac{sT}{2}} \tag{2.41}$$

The equation (2.41) provides a more accurate first-order approximation than the equation (2.36).

Another method is trapezoidal integration. Given

$$y(x) = \int_{x_0}^{x_1} f(x)\,dx \tag{2.42}$$

It can be approximated with a trapezoid

$$y(x) = \int_{x_0}^{x_1} f(x)\,dx \approx (x_1 - x_0)\left[\frac{f(x_0)+f(x_1)}{2}\right] \tag{2.43}$$

$$y(x_1) \approx (x_2 - x_1)\left[\frac{f(x_1)+f(x_2)}{2}\right] + y(x) \tag{2.44}$$

Now, it can be generalized to any point x_k

$$y_k = \Delta x\left[\frac{x_{k-1}+x_k}{2}\right] + y_{k-1} \tag{2.45}$$

Apply integration to the system

$$G(s) = \frac{Y(s)}{X(s)} = \frac{1}{s} \tag{2.46}$$

Take inverse Laplace transform to equation (2.46)

$$y(t) = \int_0^t x(t)\,dt \tag{2.47}$$

Break up by sample periods, T

$$y(kT) = \int_0^{kT} x(t)\,dt \tag{2.48}$$

Separate into two integrals

$$y(kT) = \int_{kT-T}^{kT} x(t)\,dt + \int_0^{kT-T} x(t)\,dt \tag{2.49}$$

It can be seen that equations (2.45) and (2.49) represents the sum of new and old area.

$$y(kT) \approx T\left[\frac{x(kT)+x(kT-T)}{2}\right] + y(kT-T) \tag{2.50}$$

$$y(k) = y_{k-1} + \frac{T}{2}(x_k + x_{k-1}) \tag{2.51}$$

Take Z- transformation

$$y(z)(1 - z^{-1}) = \frac{T}{2}x(z)(1 + z^{-1}) \tag{2.52}$$

Rearrange to get transfer function

$$\frac{Y(z)}{X(z)} = \frac{T}{2}\frac{(z+1)}{(z-1)} \tag{2.53}$$

$$\frac{Y(s)}{X(s)} = \frac{1}{2} \approx \frac{T}{2}\frac{(z+1)}{(z-1)} \tag{2.54}$$

$$s = \frac{2}{T}\frac{(z-1)}{(z+1)} \tag{2.55}$$

Equation (2.55) represents the bilinear transform approximation of differential equations using trapezoidal integration.

A discrete-time PID controller was proposed by Ibrahim A. El- Sharif et al., 2014. The purpose of this study was the comparison between PID controllers in continuous-time and discrete-time. **Figure 2.18** represents the block diagram of the digital control system in this experiment.

Figure 2.18

The Main Structure of Digital Control System

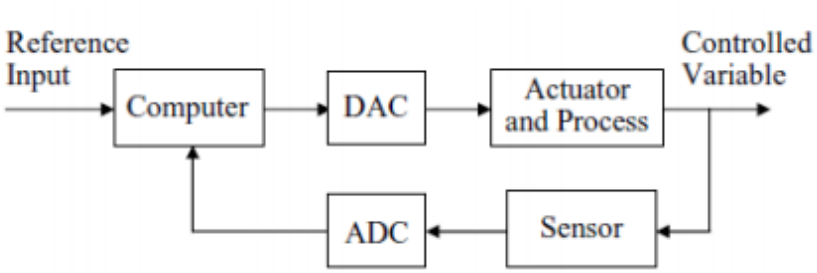

The discretization used in this study was zero-order hold and Tustin's rule to compare the performance of discrete PID controller with the one with continuous time. The closest result to the continuous response is the one provided by the Tustin method as shown in **Figure 2.19**.

Figure 2.19

The Comparison of the Response between Two Digital Compensators and a Continuous Compensator

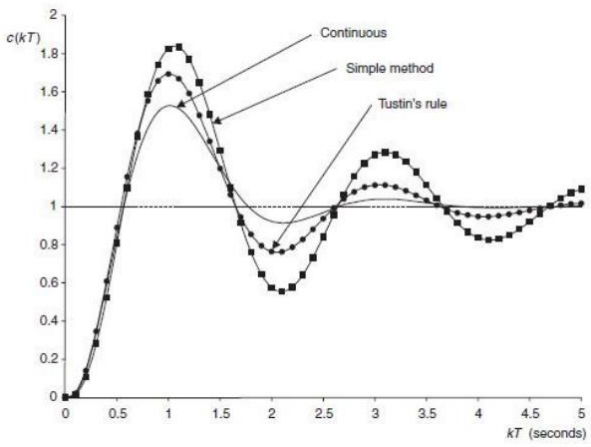

Furthermore, the response of the analog and digital PID controller is compared in **Figure 2.20**. Both designs had adequately fast response times. However, its damping ratio was less than the designated one.

Figure 2.20

Response Time of Digital PID Design

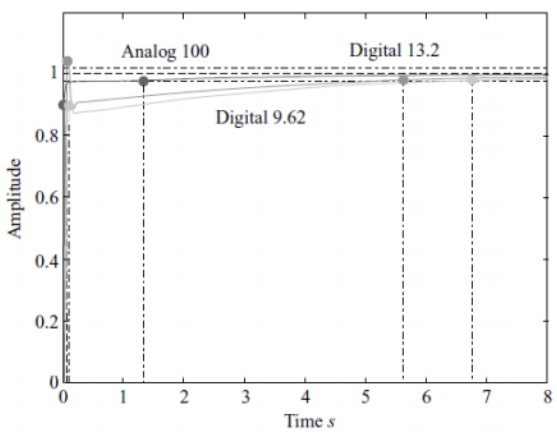

As a result, there were several benefits provided from using digital instead of a continuous PID controller. The advantages that can be made from digital PID controllers were accuracy, implementation errors, flexibility, speed, and cost. Thus, a digital controller was one of the choices when the system was needed to be controlled instead of using only a continuous-time domain. Moreover, Tustin's rule shows that it was one of the most reliable techniques to discretize the continuous time-domain into discrete-time-domain.

2.11 The Dynamic Model of a Pneumatic Actuator

Due to the nonlinearities from the compressible fluid, behavior of valve, and thermodynamics, the approximation of a dynamic model of a linear pneumatic actuator is complex. Besides, the mass flow rate through the valve is another difficulty because it is a nonlinear function of the servo valve input voltage.

A dynamic model of the pneumatic system was studied in the position control of a pneumatic actuator. The paper proposed by K. Hamiti et al., 1996. The study was about the position control of a pneumatic actuator. Before the dynamic model of the pneumatic system could be derived, the system assumed an adiabatic system, and air

performed as an ideal gas. Furthermore, the relation between the mass flow rate of the air and the change of the pressure in the chambers can be made by applying the energy conservation law. As a result, the dynamic model represents the pneumatic system obtains as a third-order transfer function. The mathematical model expresses the pneumatic plant is shown below:

$$G_p(s) = \frac{\Delta y(s)}{\Delta u(s)} = \frac{k_2}{s\left(s^2 + \frac{C}{M}s + k_1\right)} \tag{2.56}$$

where

$$k_1 = \frac{\gamma}{M}\left(\frac{S_p^2 P_{pO}}{V_{pO}} + \frac{S_n^2 P_{nO}}{V_{nO}}\right)$$

$$k_2 = \frac{\gamma R T_s G_i}{M}\left(\frac{S_p}{V_{pO}} + \frac{S_n}{V_{nO}}\right) \tag{2.57}$$

where y(s) is position output of the piston, u(s) is the input voltage to the valve, γ is specific heat ratio of air, C is the viscosity coefficient, M is piston mass, T_s is supplied air temperature, R is gas constant. S, V, and P are the area of the piston, volume, and pressure in each chamber. Also, subscript p and n denote chamber p and n of the piston and O denote to operation point. Last, G_i is the linearized air mass flow rate coefficient. It was difficult to measure all unknown parameters in equation (2.56). Furthermore, there is a pole at the origin point in equation (2.56) which makes it harder to identify the transfer function. As a result, the dynamic model in equation (2.56) was modified to eliminate the pole at origin and the effects of uncertainties by adding a proportional controller to the system and called it an inner loop as shown in **Figure 2.21**. The Chien-Hrones-Reswick (Table 2.1) was used to tune for the PI parameter to control the modified plant, this loop was called the outer loop.

Figure 2.21

Analog Inner Loop Block Diagram

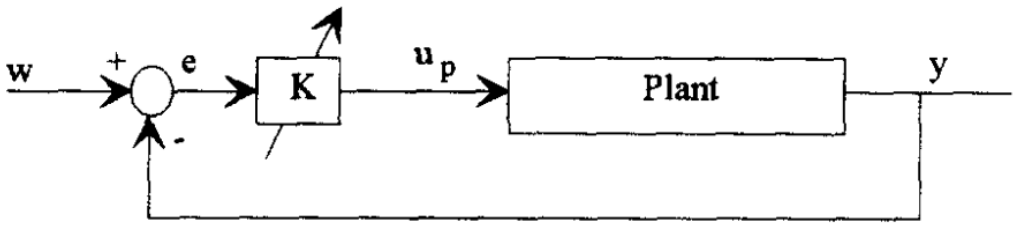

Table 2.1

Chien-Reswick Tuning Formulas

Controllers		Overshoot = 0%	
Type	Parameters	Regulation	Tracking
PI	K_P	$0.6\frac{T}{\tau}$	$0.35\frac{T}{\tau}$
	T_I	$4\,\tau$	1.2T

However, the integrator causes the system to stick and slip near the desired location due to the presence of stiction. In order to achieve a good steady-state accuracy, the integral gain weighted by a function $\alpha(f)$ is needed to eliminate the limit cycle. The experimental result was separated into 5 cases. First, the controller without the auxiliary block $\alpha(f) = 1$ for all errors is designed in this experiment. Due to the lack of the function $\alpha(f)$, the system never appointed to the desired location due to stiction that could not be represented in the plant model as shown in **Figure 2.22**.

Figure 2.22

The Resulting Step Response when the Stiction at Low Velocity is Applied

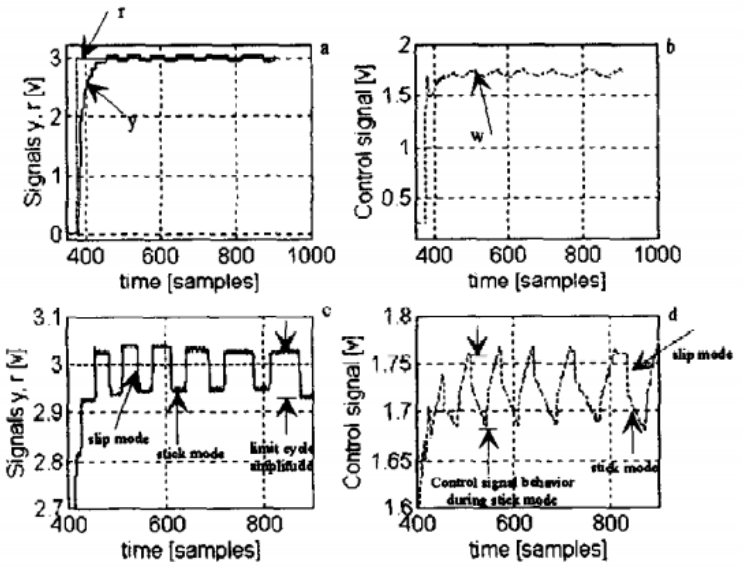

Second, the test was designed to verify the ability to progressively eliminate the limit cycle of the auxiliary block. **Figure 2.23** represented that the target location was reached, the control signal then stays constant. Since the weighting factor was small, the integral part did not affect.

Figure 2.23

The Step Response when the Automatic Tuning is Used

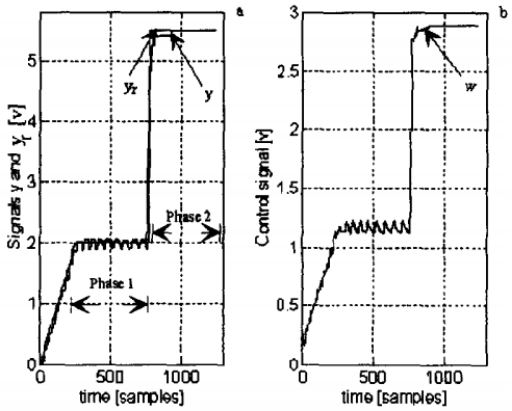

Third, variation in load mass was considered in order to verify the robustness of the control strategy. **Figure 2.24** clearly shown that the additional load mass could not affect the responses of the system.

Figure 2.24

The Step Response when the 12 kg is Added in Curve a, and 0.4 kg is Added in Curve b

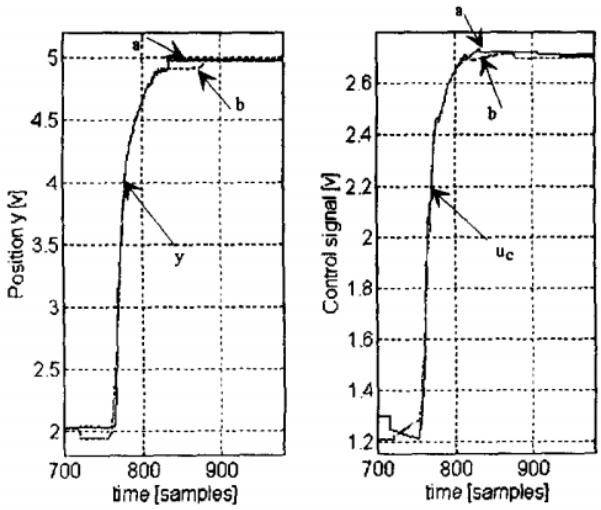

Fourth, the disturbance rejection ability was to be validated by moving the load jerkily from the steady-state point. **Figure 2.25** illustrated that the position with the proposed controller well performed even the integral part behaved worse. Thus, it can be summarized that the proposed controller had good disturbance rejection.

Figure 2.25

The Step Response when External Load Disturbance is Applied

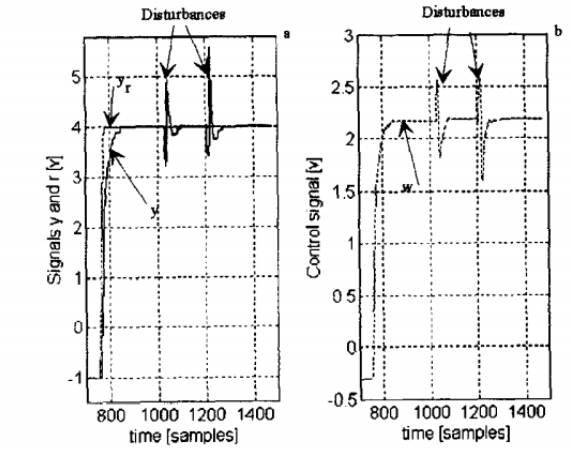

Last, an ability to track the non-periodic path of the system was conducted. It could be seen in **Figure 2.26** that good tracking was maintained even on an arbitrary path. However, the system overshot the final value when the relatively fast motion was applied.

Figure 2.26

The System with an Arbitrary Non Periodic Path and the Curve Tracking of the Control Signal

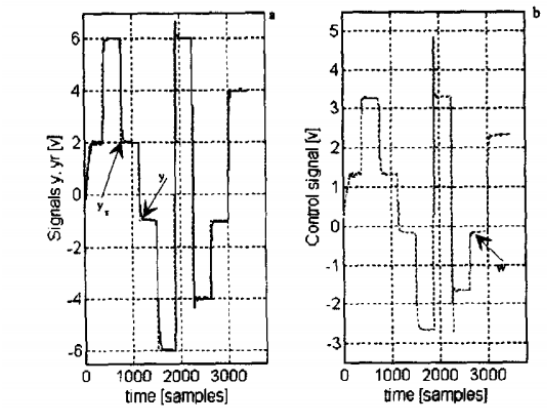

To conclude, the complexity of the pneumatic plant model can be reduced by modifying the system with a proportional controller to eliminate the pole at the origin. Moreover, nonlinearities and stabilizes can be handled with an integrator. The integral weighting provided significant output to eliminate the limit cycle. Thus, the tuned PI controller gave a good location response as well as the additional load mass as a disturbance response. Finally, the control strategy could be applied with various PI and PID formulas to produce the desired motion.

CHAPTER 3
METHODOLOGY

3.1 Concept

The position control of the pneumatic actuator by a robust controller with a full-order H-infinity optimal control method is proposed. The controller is directly derived by H_∞ synthesis as a high-order controller. In the beginning, the weigh function is predefined by the Automatic weight selection algorithm. Then, H-infinity synthesis is implemented to compute for the optimal controller which the resulting gamma minimizes the infinity norm. Even though the infinity norm is difficult to compute, MATLAB has a tool to solve it called hinfopt. As a result, a robust controller is computed for a multivariate feedback control system represented as a controller transfer function. Finally, the bilinear transformation is applied to transform the continuous-time controller transfer function into a discrete-time transfer function.

3.2 Experimental Design

This thesis is focusing on position controller design by H-infinity synthesis and PID controller based on pole placement tuning method. Then, the performance of each controller will be compared. The system is designed as shown in **Figure 3.1**.

Figure 3.1

Experimental Setup of the Pneumatic System

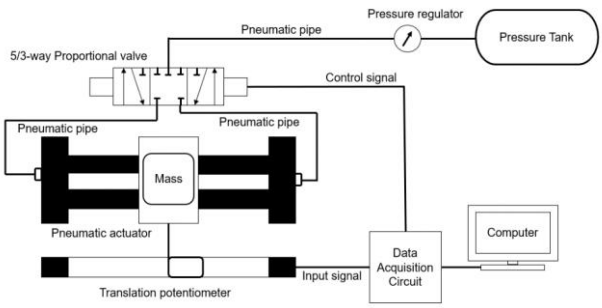

3.3 Equipment Selection

The selected piston is a magnetically coupled rodless cylinder as presented in **Figure 3.2**. A low friction pneumatic cylinder SMC CDY1S10H has specifications described in Table 3.1. The valve used in this experiment is a 5/3-way proportional valve MPYE-5-1/8-HF-010B to control the extrusion and intrusion movement of the cylinder depicted in **Figure 3.3**. Moreover, the specification of this valve is represented in Table 3.2. The sensor used in this study is a linear displacement encoder MLO-POT-500-TLF shown in **Figure 3.4**. Finally, the selected microcontroller to control the valve is the Arduino Due (Table 3.3) shown in **Figure 3.5**

Figure 3.2

Magnetically Coupled Rodless Cylinder

Figure 3.3

Proportional Directional Control Valve

Figure 3.4

Displacement Encoder

Figure 3.5

Microcontroller

Table 3.1

Piston's Specifications

Slider type	Slide Bearing
Bore size	10 mm
Maximum working pressure	7 bar (0.7 MPa)
Speed of the piston	50 to 400 mm/s
Standard stroke	500 mm

Table 3.2

Valve's Specifications

Valve type	Proportional directional control valve
Function of the valve	5/3-way
Setpoint value input	Analog voltage signal
Nominal size	6 mm
Nominal flow rate	700 l/min
Power supply	17-30 V DC
Setpoint value	0-10 V
Valve mid-position	5 (±0.1) V DC

Table 3.3
Sensor's Specifications

Encoder type	Analogue displacement encoder
Measuring principle	Potentiometric
Stroke length	500 mm
Resolution	0.01 mm
Max. speed of travel	10 m/s
Max acceleration	200 m^2/s

Table 3.4
Microcontroller's Specifications

Operating voltage	3.3 V
Supply voltage	7-12 V
SRAM	96 KB
Clock speed	84 MHz

3.4 System Identification

According to equation (2.56), there are several unknown parameters needed to be identified. Thus, to simplify the calculation, the dynamic model is estimated as the second order of strictly proper transfer function. The model is presented as the following equation:

$$\frac{y(s)}{u(s)} = \frac{b_1 s + b_0}{s^2 + a_1 s + a_0} \tag{3.1}$$

where

b_1, b_0, a_1, and a_0 are constant real numbers.

The unknown parameters in equation (3.1) can be identified via the system identification App in MATLAB. The objective of this app is to estimate and validate the linear model from Single-input/Single-output (SISO) data. The process of the linear model estimation can be written in steps.

1. Import input and output data to the System Identification app. Time-domain data is used to estimate the linear model by specifying the initial and sample time of the data.
2. Remove the mean of input and output by subtracting by its mean. As a result, the data has a zero-mean value.

3. Order of poles and zeros of the desired transfer function are specified as non-negative number. Then, the transfer function is estimated as a continuous-time domain.

3.4.1 Time-domain Data Estimated for the Continuous-time Transfer Function

The estimation algorithms are different depending on several factors. In this paper, by specifying the initial and sample time of the input and output data, time-domain data can be used to estimate for a plant model in the continuous-time domain. There are two main parts in the estimation using Time-Domain data. The first one is parameter initialization, and the second one is parameter update.

Initially, the algorithm estimates the parameters via the Instrument Variable method. Prefiltered data is used by the State-Variable Filters (SVF) approach and the Generalized Poisson Moment Functions (GMPF) approach to estimate a continuous-time parameter. The simplified refined method (SRIVC) has a prefilter which is the denominator initialized with the SVF of the current model. The prefilter iterates until it reaches the defined maximum iterations, or the model change is less than the desired tolerance.

In parameter update, the nonlinear least-squares search method is used to update the initialized parameter. In addition, the objective of this searching technique is to minimize the weight prediction error norm.

3.5 PID Controller based on Pole Placement Tuning

The Pole placement method is a method to place closed-loop poles of a plant at the desired location in the s-plane. The system response depends on the poles' location. If the poles are placed further from the Imaginary axis, the speed of the response will be fast. On the other hand, the further the poles from the Real axis, the more system oscillation frequency. From **Figure 2.6** the PID controller can be expressed as:

$$G_C(s) = K_P + \frac{K_I}{s} + K_D s \qquad (3.2)$$

A closed-loop transfer function can be written as:

$$T_C(s)= \frac{G_C(s)G(s)}{1+G_C(s)G(s)} \quad (3.3)$$

The value of K_P, K_I, and K_D by pole placement method is calculated by equating the characteristic equation of the closed-loop transfer function with the location of available poles.

The location of the poles can be done based on the relationship between the voltage and error of the system.

Figure 3.6

Pole Location Selection

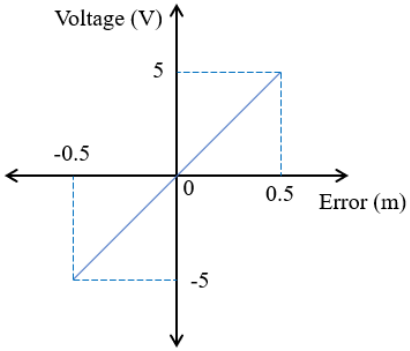

The maximum possible error of the pneumatic actuator is 0.5 m because its maximum stroke length is 0.5 m. While the range of the applied voltage to the valve is 0 to 10 V. In addition, the voltage 0 to 5 V is used to move the piston from the left to the right side. On the other hand, to move the piston from the right-hand side to the left, voltage 5 to 10 V is applied. After removing the means value, the relation between the supplied voltage and error can be presented as shown in **Figure 3.6.** The acceptable proportional gain must lie on this linear function as expressed in the equation below.

$$\text{Voltage} = \text{error} \times K_P \quad (3.4)$$

At the maximum error of 0.5 m, the system must provide the maximum voltage of 5.0 V either. As a result, the location of the poles that make the proportional gain approximately equal to 10 is acceptable.

3.6 Optimal Control Theory

Optimal control theory is the optimization process to deal with the control for a dynamic system. In other words, the system with multiple-input or multiple-output provides infinite solutions. To obtain the best solution that minimizes the cost function, the optimal control theory must be applied to the system.

3.7 γ-Iteration of H_∞ Synthesis (hinfopt)

This is the command in MATLAB to calculate for the optimal controller via H-infinity γ-iteration. The two-Riccati formulae are solved to find the optimal γ so that they provide the cost function in equation (2.23) under desired tolerance. The H-infinity theory uses a reliable procedure to design for the robust controller. This method satisfies singular value loop shaping specifications optimally. The benefits and drawbacks of using H-infinity methods over other methods are summarized in Table 3.5.

Table 3.5

Summarize Advantages and Disadvantages of each Technique

Methods	Advantages	Disadvantages
H_∞	Stability and sensitivity meet the requirement	The resulting controller is calculated as a full order,
	Readily available method	the designer needs some understanding of mathematic.
H_2	Stability and sensitivity are focused on designing	It may take several iterations in computation
	Guaranteed the stability of the closed loop	
LQR	Provide a good stability margin	full-state feedback is required
	Only focus on the controller gain	The exact plant model is required
		Can take many iterations

Methods	Advantages	Disadvantages
LQG	The noises are used in calculation	Stability margin cannot be sure
		Need exact plant model
		Can take many iterations
LQG/LTR	Provide a good stability margin	The resulting controller has high gain
μ synthesis	The structured/ unstructured uncertainty is combined in designing process	Controller size is huge

CHAPTER 4
RESULT AND DISCUSSION

4.1 Overview

This section presents the step-responses simulation and bode plot of the proposed conventional H-infinity controller compare with the PID controller based on the pole placement tuning method. Furthermore, the experimental output from the position control of the pneumatic system is represented to verify the robustness of the proposed controller by varying load mass to 3 kg and supply pressure is adjusted to 1, 4, and 5 bar (0.1, 0.4, and 0.5 MPa).

4.2 Evaluation and Validation Data

For this experiment, the dynamic model of the pneumatic system is determined with the supplied of 4 bars (0.4 MPa) without additional load mass applied to the piston. The valve is controlled by Arduino due by supplying the analog input voltage to control the direction of the pneumatic actuator. The generated voltage is between 0-10 V. The input voltage to the valve and the position of the cylinder are measured to investigate the relation between these data. Two sets of data have been collected separately as evaluation data and validation data, depicted in **Figure 4.1** and **Figure 4.2,** respectively.

The input voltage is generated every 0.01 s. Thus, the sampling time in the identification is 0.01 s. The evaluation data is a set of data used to identify unknown parameters of the desired transfer function, while the validation of the estimated transfer function is done by the validation data. The validation data is used to determine the correctness of the estimated model. Moreover, the data at which the piston hit with both ends is unacceptable to use as evaluation and validation data. The mean value of these data is to be removed before it can be used to identify the plant model.

Figure 4.1

Evaluation Data

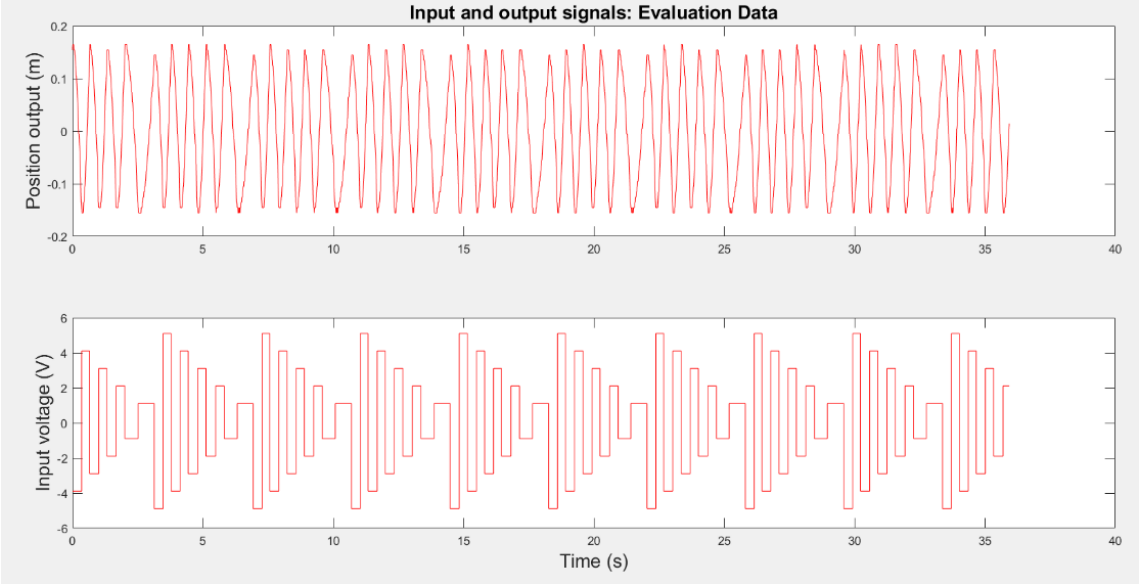

Figure 4.2

Validation Data

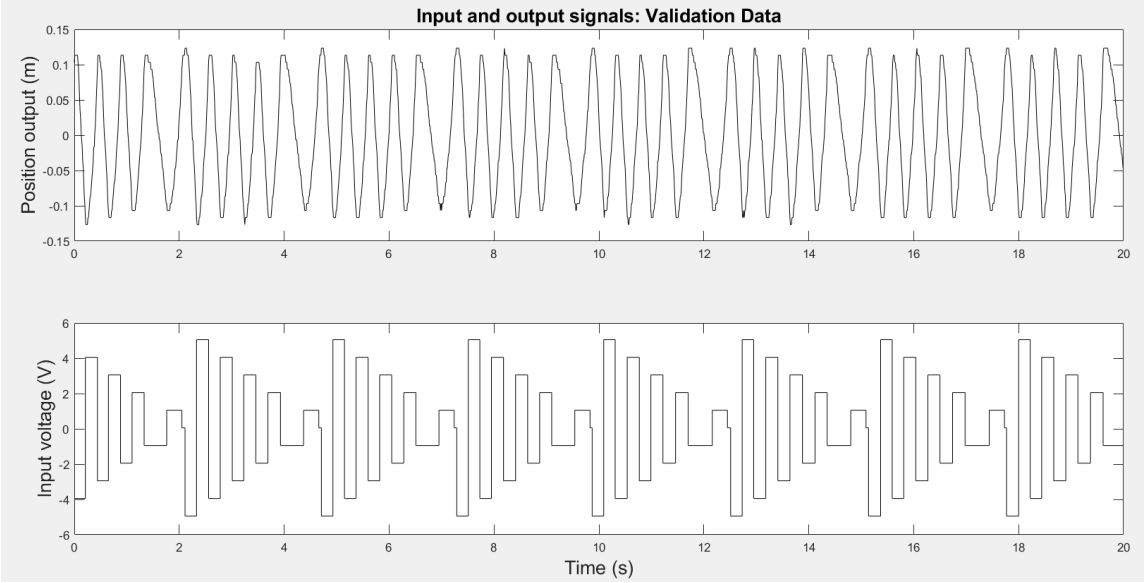

4.3 Plant Model from System Identification

After obtains the evaluation data and validation data, the system identification on MATLAB is applied to identify the plant model. The starting time of the data has been set at 0 s. By specifying the number of zero as one and the number of poles as two the estimated plant transfer function obtains as equation (4.1). **Figure 4.3** depicts the comparison between the experimental output from the measurement with the simulated output from the estimated model.

$$G_p(s)= \frac{-0.2415s+2.473}{s^2+10.95s+104.2} \tag{4.1}$$

Figure 4.3

Comparison of the Model and Measured Output

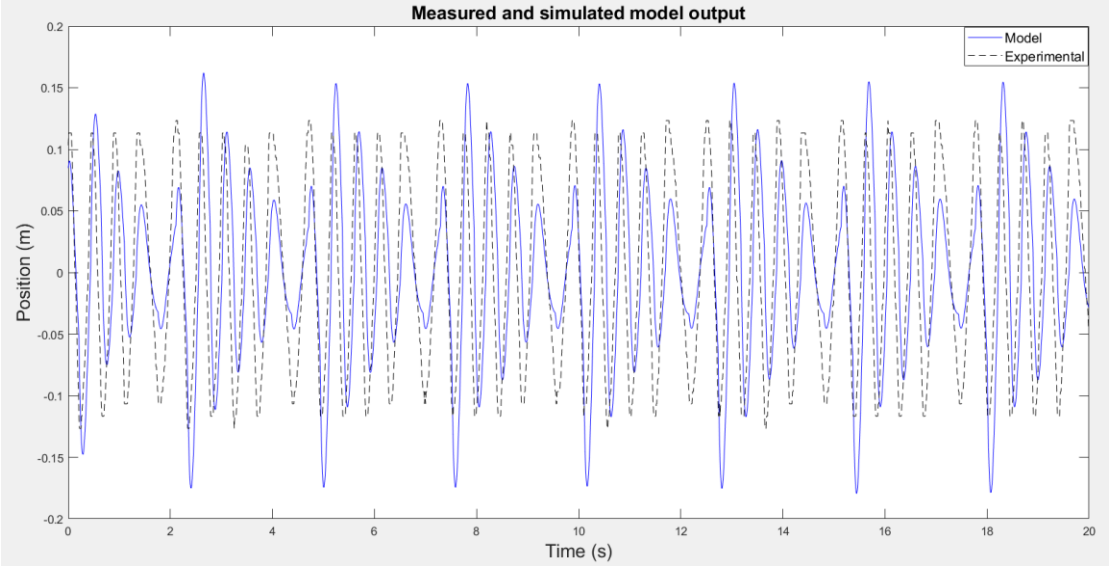

4.4 PID Controller based on Pole Placement Tuning Method

According to the strictly proper transfer function of the plant is defined as equation (4.1). Initially, the poles of the plant are located at -5.47+8.62j and -5.47-8.62j as shown in **Figure 4.4**.

Figure 4.4

Location of Poles and Zero of the Plant

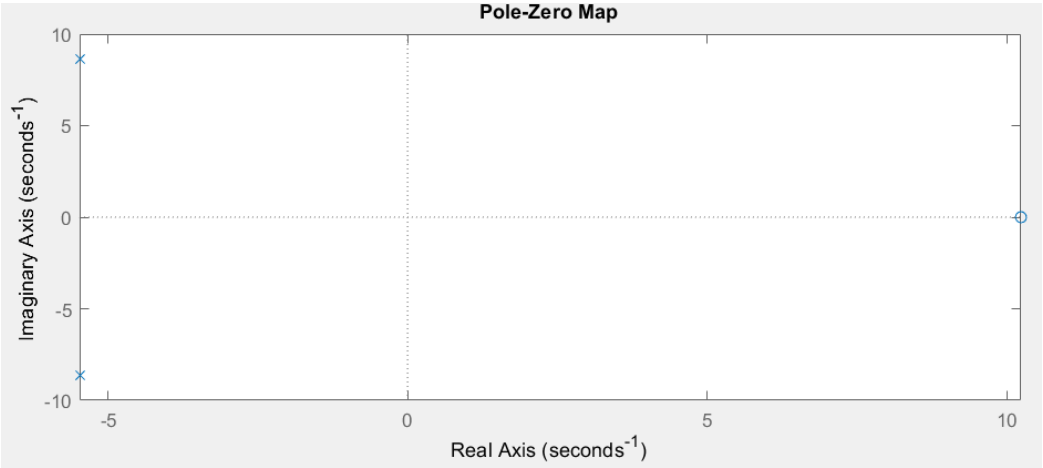

The derivative first-order PID controller is tuned based on the pole placement tuning method. Equation (3.2) represents the structure of the controller. **Figure 3.6** describes that the allowable K_p gain must lie on the linear function between position error and supplied voltage. Therefore, the proportional gain is selected approximately equal to 10.0. The poles at which provide the desired proportional gain are selected as -5.5, -5.5+7.1j, and -5.5-7.1j. As a result, by equating the poles' location with the closed-loop characteristic equation, the PID controller gain is obtained as equation (4.2).

$$G_C(s)=10.1453+\frac{125.7199}{s}+1.2388s \qquad (4.2)$$

Figure 4.5

Desired Poles' Location for Tuning PID Controller

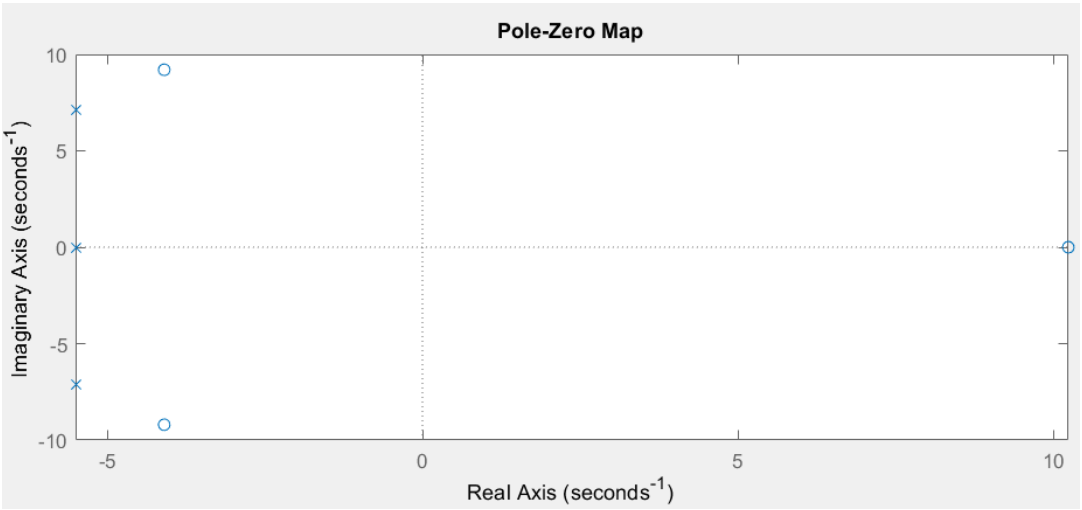

4.5 Weighting Function

To compare with the PID controller, a conventional H-infinity optimal controller is proposed. The weighting function must be determined before the conventional H-infinity controller is designed. The weighting functions which meet all requirements have the crossover frequency at 4.0 rad/s and they are represented as:

$$W_1 = \frac{0.5s+4.0}{s+0.04},\ W_2 = \frac{s+100}{s+200} \tag{4.3}$$

These weighting functions are used to improve robustness and performance. **Figure 4.6** shows the bode diagram of the inverse of both weighting functions. **Figure 4.7** depicts that the Sensitivity function (S) is lower than $\frac{1}{W_1}$ for every frequency. Also, **Figure 4.8** illustrates that all Complementary sensitivity function (T) is lower than $\frac{1}{W_2}$ for every frequency. Last, **Figure 4.9** presents the Sensitivity and Complementary sensitivity function. At the crossover frequency of 4.0 rad/s, the value of S and T should be less than 1.0.

Figure 4.6

Inverse Weighting Functions

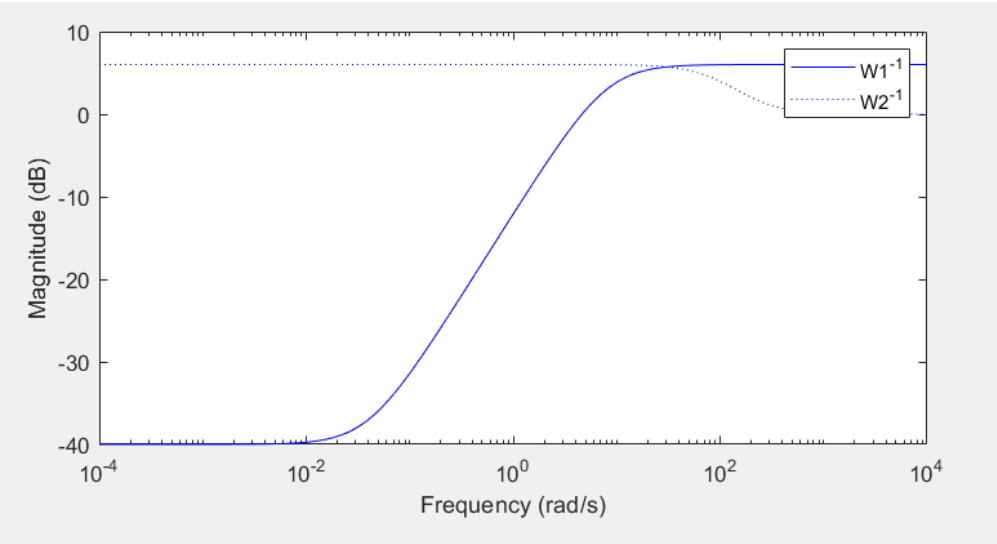

Figure 4.7

Comparison between Sensitivity Function (S) and Inverse of W_1

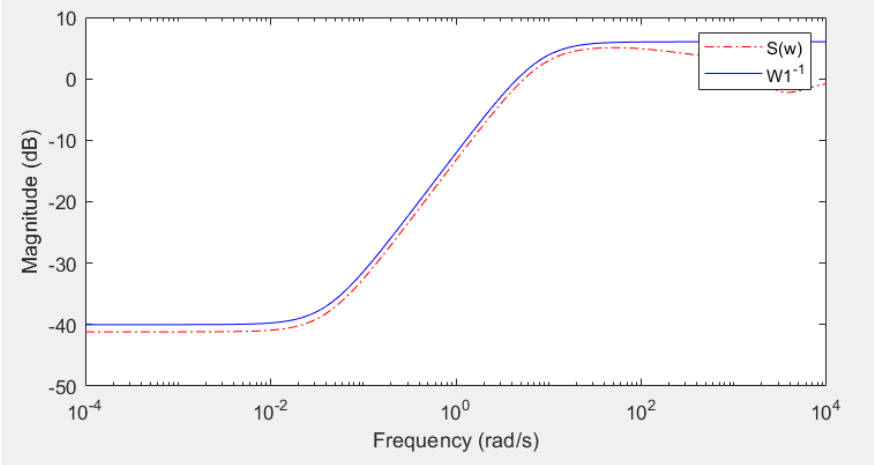

Figure 4.8

Comparison between Complementary Sensitivity Function (T) and Inverse of W_2

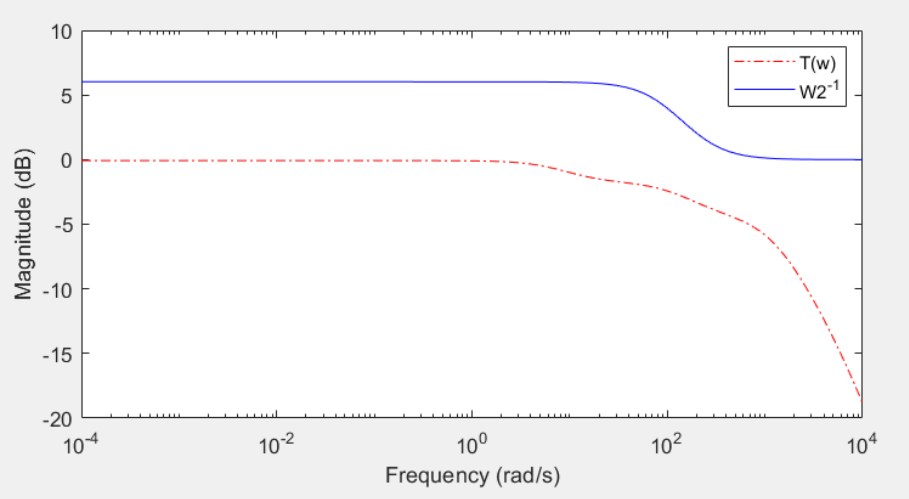

Figure 4.9

Bode Magnitude of S(s) and T(s)

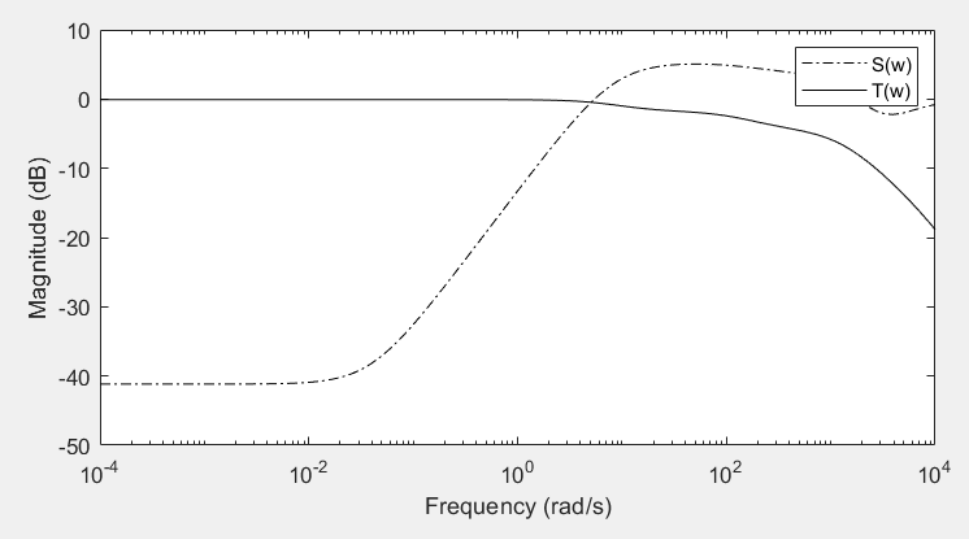

4.6 Augmented Plant

After the weighting functions are obtained, the plant is augmented to form an augmented plant. There are 2 inputs and 3 outputs from the augmented plant. They can be expressed as equations (4.4) to (4.9).

From input 1 to output:

$$1: \frac{0.5s+4.0}{s+0.04} \tag{4.4}$$

$$2: 0 \tag{4.5}$$

$$3: 1 \tag{4.6}$$

From input 2 to output:

$$1: \frac{0.1207s^2-0.2705s-9.892}{s^3+10.99s^2+104.6s+4.168} \tag{4.7}$$

$$2: \frac{-0.2415s^2-21.68s+247.3}{s^3+210.9s^2+2294s+20840} \tag{4.8}$$

$$3: \frac{0.2415s-2.473}{s^2+10.95s+104.2} \tag{4.9}$$

This augmented can be transformed into state-space form as follows:

$$P(s) = \begin{bmatrix} A & B \\ C & D \end{bmatrix} \tag{4.10}$$

Where,

A=

$$\begin{bmatrix} -0.0400 & 0 & 0 & 0 & 0 & 0 & 0 & 0 & 0 \\ 0 & -10.9900 & -13.0798 & -1.0420 & 0 & 0 & 0 & 0 & 0 \\ 0 & 8.0000 & 0 & 0 & 0 & 0 & 0 & 0 & 0 \\ 0 & 0 & 0.5000 & 0 & 0 & 0 & 0 & 0 & 0 \\ 0 & 0 & 0 & 0 & -210.9500 & -35.8469 & -20.3516 & 0 & 0 \\ 0 & 0 & 0 & 0 & 64.0000 & 0 & 0 & 0 & 0 \\ 0 & 0 & 0 & 0 & 0 & 16.0000 & 0 & 0 & 0 \\ 0 & 0 & 0 & 0 & 0 & 0 & 0 & -10.9500 & -13.0250 \\ 0 & 0 & 0 & 0 & 0 & 0 & 0 & 8.0000 & 0 \end{bmatrix}$$

$$B=\begin{bmatrix} 2 & 0 \\ 0 & 2 \\ 0 & 0 \\ 0 & 0 \\ 0 & 1 \\ 0 & 0 \\ 0 & 0 \\ 0 & 1 \\ 0 & 0 \end{bmatrix}$$

$$C=\begin{bmatrix} 1.9900 & 0.0604 & -0.0169 & -1.2365 & 0 & 0 & 0 & 0 & 0 \\ 0 & 0 & 0 & 0 & -0.2415 & -0.3387 & 0.2415 & 0 & 0 \\ 0 & 0 & 0 & 0 & 0 & 0 & 0 & 0.2415 & -0.3091 \end{bmatrix}$$

$$D=\begin{bmatrix} 0.5000 & 0 \\ 0 & 0 \\ 1.0000 & 0 \end{bmatrix}$$

4.7 H-infinity Controller

H-infinity optimal control synthesis via γ-iteration is applied to solve for the optimal H-infinity controller using two-Riccati equations. The optimal γ is found to be 0.9922. The resulting optimal H-infinity controller is:

$$K(s)=\frac{\begin{array}{c}-5000s^9+(1.543x10^7)s^8+(3.827x10^9)s^7 \\ +(1.196x10^{11})s^6+(2.362x10^{12})s^5+(2.826x10^{13})s^4 \\ +(2.391x10^{14})s^3+(1.211x10^{15})s^2 \\ +(3.802x10^{15})s+(1.502x10^{14})\end{array}}{\begin{array}{c}s^9+5041s^8+(1.145x10^7)s^7 \\ +(2.058x10^9)s^6+(4.348x10^{10})s^5+(6.228x10^{11})s^4 \\ +(4.297x10^{12})s^3+(1.997x10^{13})s^2 \\ +(1.577x10^{12})s+(3.14x10^{10})\end{array}} \quad (4.11)$$

4.8 Step Response and Bode Plot

After the conventional H-infinity controller has been calculated, the step response and bode plot of closed-loop feedback of PID controller and H-infinity controller are compared in **Figure 4.10** and **Figure 4.11**, respectively. From the step response of the PID controller, the Settling time is 0.747 s, and the final value of 1. While the H-infinity controller provides the Settling time of 0.478 s with the final value of 0.991. Furthermore, the bode diagram presents the gain and phase margin of the PID controller and H-infinity controller as 7.39dB, -180 deg, and 2.26 dB, infinite deg, consecutively.

Figure 4.10

Step Responses of the PID based on Pole Placement Tuning Method and Proposed H-infinity Controllers

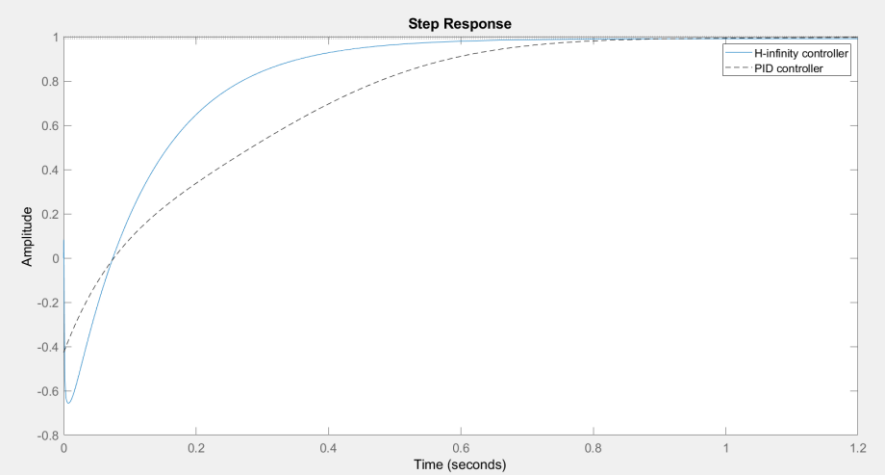

Figure 4.11

Bode Plot of PID and Proposed H-infinity Controllers

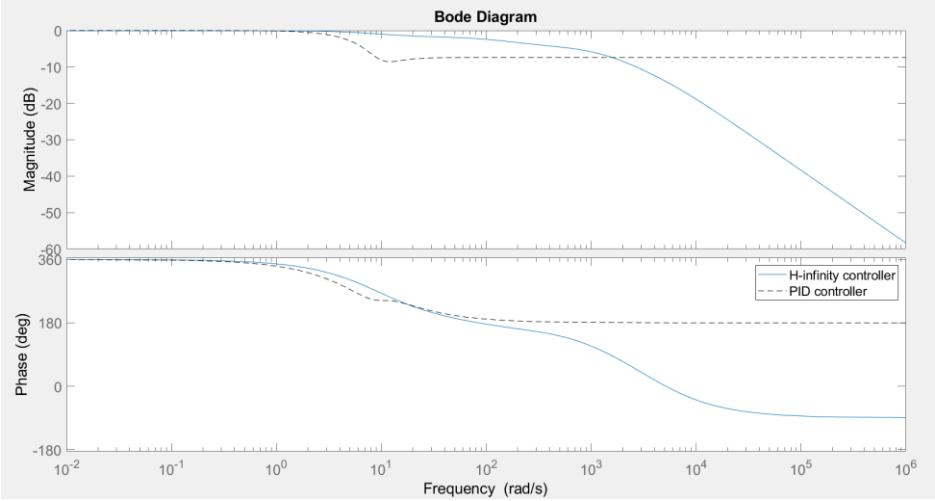

4.9 Discretization

Later than the proposed controller is obtained, Bilinear transform is used to discretize the continuous-time domain controller transfer function to the discrete-time domain. The relation between the s-domain and z-domain transfer function is represented as the equation (2.55). The sample time of discretization is 0.1 s. As a result, the controller transfer function in discrete time is shown as:

$$K(z)= \frac{\begin{matrix}64.29z^9-104.1z^8+9.531z^7\\ +115.5z^6-126.2z^5+32.59z^4\\ +34.66z^3-39.02z^2+16.32z-3.252\end{matrix}}{\begin{matrix}z^9-0.8548z^8-1.802z^7\\ +2.184z^6+0.2838z^5-1.698z^4\\ +0.8634z^3+0.2491z^2-0.3448z+0.1199\end{matrix}} \tag{4.12}$$

Rearrange equation (4.12) in the form of input function (e) and output function (f),

$$K(z)=\frac{f}{e}= \frac{\begin{matrix}64.29z^9-104.1z^8+9.531z^7\\ +115.5z^6-126.2z^5+32.59z^4\\ +34.66z^3-39.02z^2+16.32z-3.252\end{matrix}}{\begin{matrix}z^9-0.8548z^8-1.802z^7\\ +2.184z^6+0.2838z^5-1.698z^4\\ +0.8634z^3+0.2491z^2-0.3448z+0.1199\end{matrix}} \tag{4.13}$$

Divided all terms by $\frac{1}{z^9}$

$$\frac{f}{e}= \frac{\begin{matrix}64.29-\frac{104.1}{z}+\frac{9.531}{z^2}\\ +\frac{115.5}{z^3}-\frac{126.2}{z^4}+\frac{32.59}{z^5}\\ +\frac{34.66}{z^6}-\frac{39.02}{z^7}+\frac{16.32}{z^8}-\frac{3.252}{z^9}\end{matrix}}{\begin{matrix}1-\frac{0.8548}{z}-\frac{1.802}{z^2}\\ +\frac{2.184}{z^3}+\frac{0.2838}{z^4}-\frac{1.698}{z^5}\\ +\frac{0.8634}{z^6}+\frac{0.2491}{z^7}-\frac{0.3448}{z^8}+\frac{0.1199}{z^9}\end{matrix}} \tag{4.14}$$

$$\begin{aligned} f(k) = {} & 0.8548f(k-1) + 1.802f(k-2) - 2.184f(k-3) - 0.2838f(k-4) \\ & + 1.698f(k-5) - 0.8634f(k-6) - 0.2491f(k-7) + 0.3448f(k-8) \\ & - 0.1199f(k-9) + 64.29e(k) - 104.1e(k-1) + 9.531e(k-2) \\ & + 115.5e(k-3) - 126.2e(k-4) + 32.59e(k-5) + 34.66e(k-6) \\ & - 39.02e(k-7) + 16.32e(k-8) - 3.252e(k-9) \end{aligned} \tag{4.15}$$

Equation (4.15) represents the output voltage to the valve f(k) at the current time, computed from the previous nine output voltage and the ten previous errors e(k) until the present time. The equation (4.15) is implemented into the hardware to control the position of the pneumatic actuator and the results are presented in the next section.

4.10 Experiment

This part shows the measurement position of the pneumatic actuator controlled by the PID and the proposed H-infinity controller. Moreover, the robustness of the controller is verified by varying load mass and supply pressure. The nominal pressure of the system is tested at 4 bar (0.4 MPa) without additional load mass to the system. The position is illustrated as shown in **Figure 4.12**.

Figure 4.12

Compare the Position of the Piston Controlled by Two Types of Controllers at a Setpoint of 0.25 m at 4 Bar (0.4MPa) Supply Pressure (Nominal Pressure)

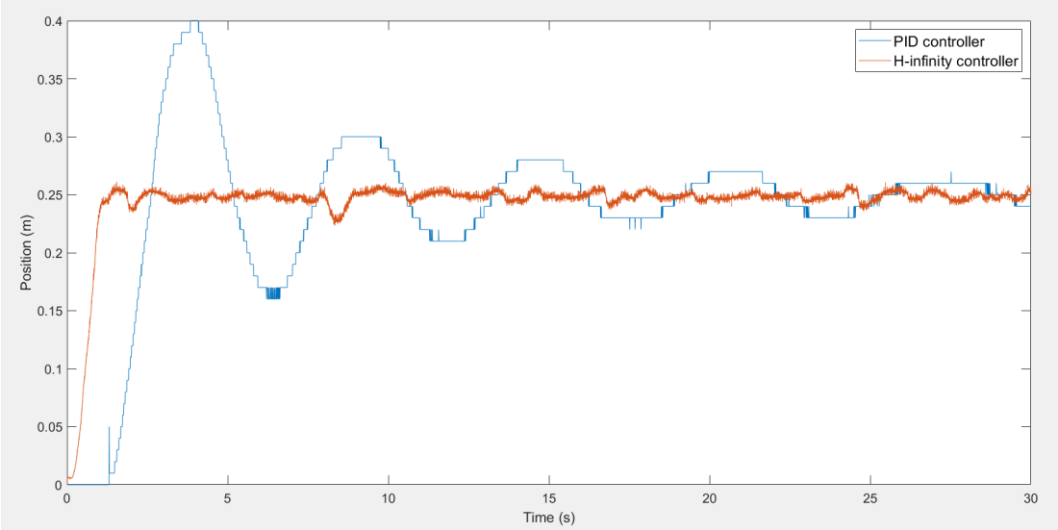

Test the robustness by changing the supply pressure to 1 and 5 bar (0.1 and 0.5 MPa). From **Figure 4.13**, it can be obviously seen that the system controlled by the H-infinity controller approaches the setpoint much faster than the PID controller. The PID controller takes approximately 5 min while the H-infinity controller takes just about 10 s. Moreover, the overshoot provided by the PID controller is extremely high. Thus, the H-infinity controller is much better than the PID controller at this level of pressure.

Figure 4.13

Compare the Position of the Piston Controlled by Two Types of Controllers at a Setpoint of 0.25 m at 1 Bar (0.1 MPa) Supply Pressure

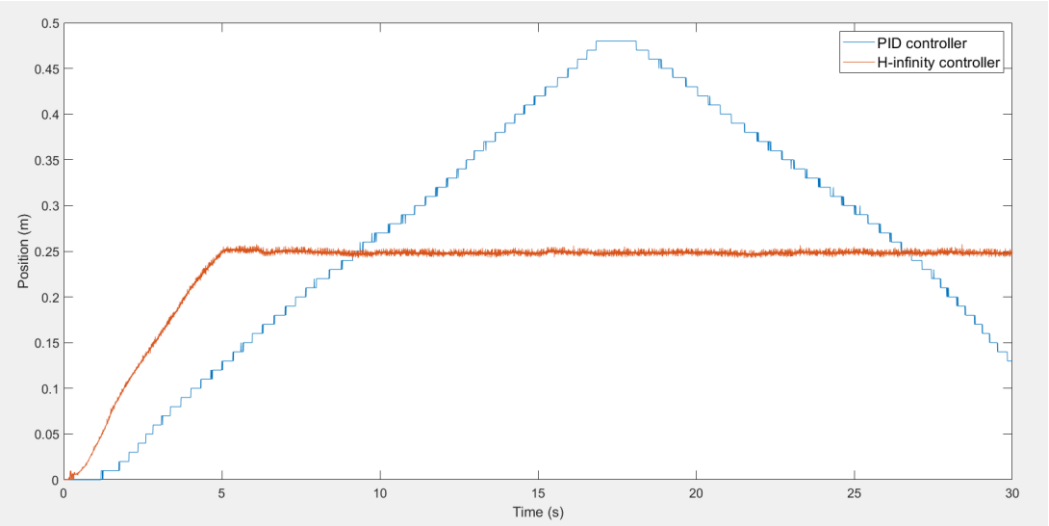

Figure 4.14

Compare the Position of the Piston Controlled by Two Types of Controllers at a Setpoint of 0.25 m at 5 Bar (0.5 MPa) Supply Pressure

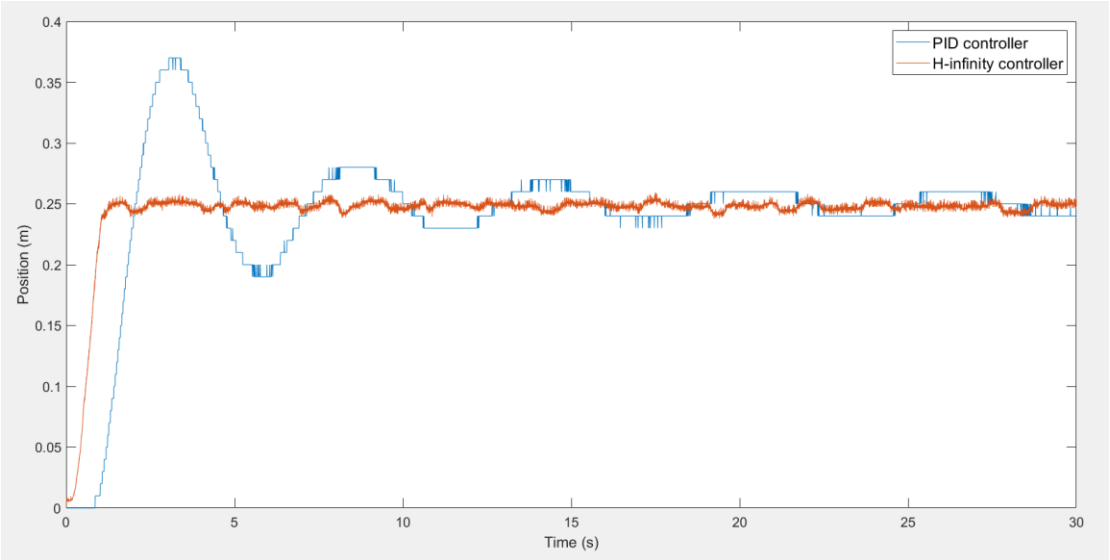

Furthermore, the system is tested with an addition of 3 kg load mass to the system to verify the robustness.

Figure 4.15

Compare the Position of the Piston Controlled by Two Types of Controllers at a Setpoint of 0.25 m with 3 kg Load Mass at 4 Bar (0.4 MPa) Supply Pressure (nominal pressure)

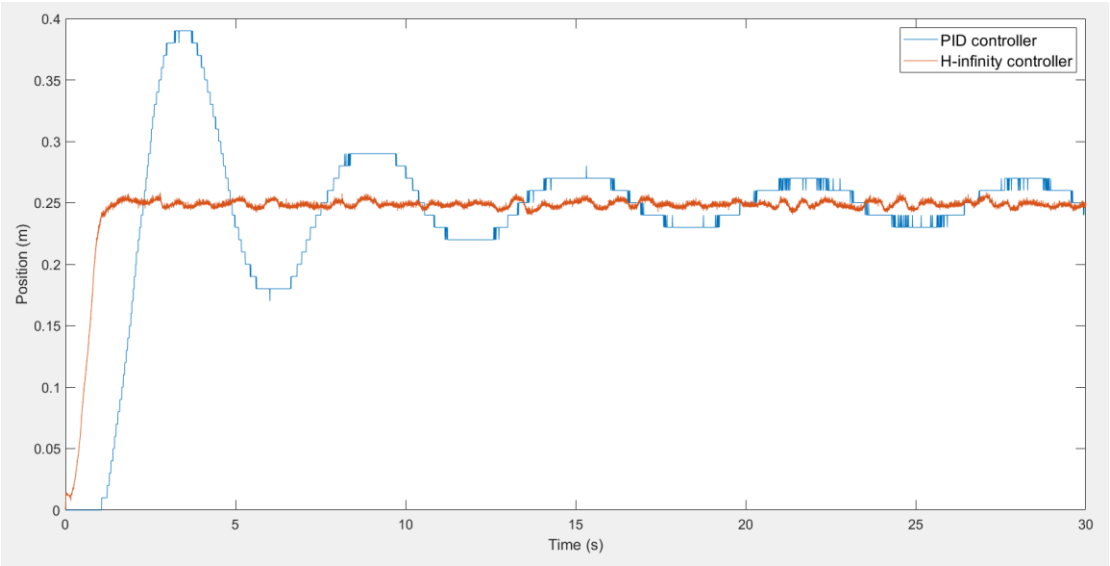

Figure 4.16

Compare the Position of the Piston Controlled by Two Types of Controllers at a Setpoint of 0.25 m with 3 kg Load Mass at 1 Bar (0.1 MPa) Supply Pressure

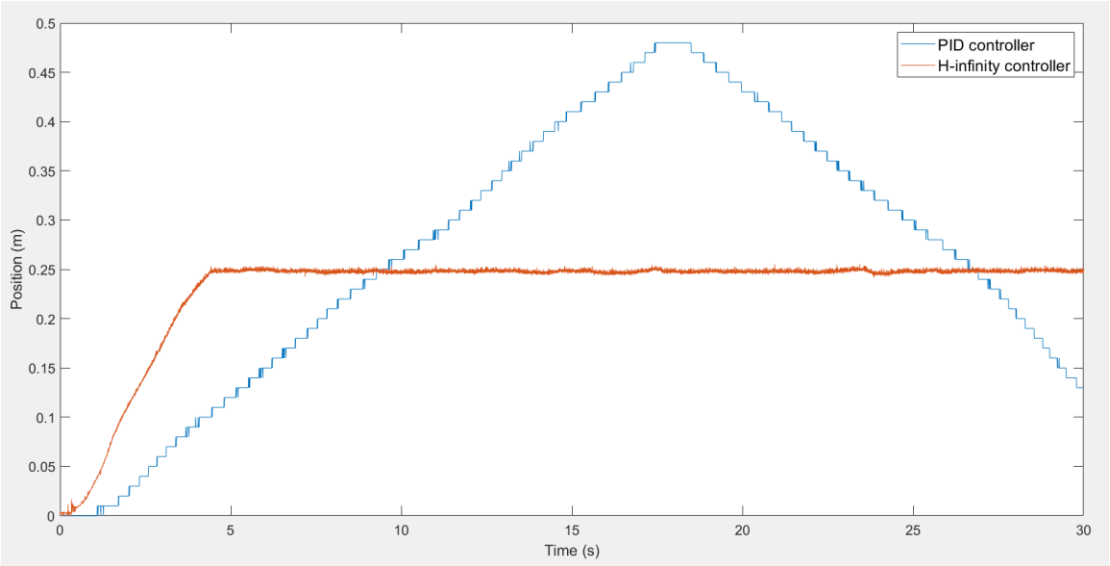

Figure 4.17

Compare the Position of the Piston Controlled by Two Types of Controllers at a Setpoint of 0.25 m with 3 kg Load Mass at 5 Bar (0.5 MPa) Supply Pressure

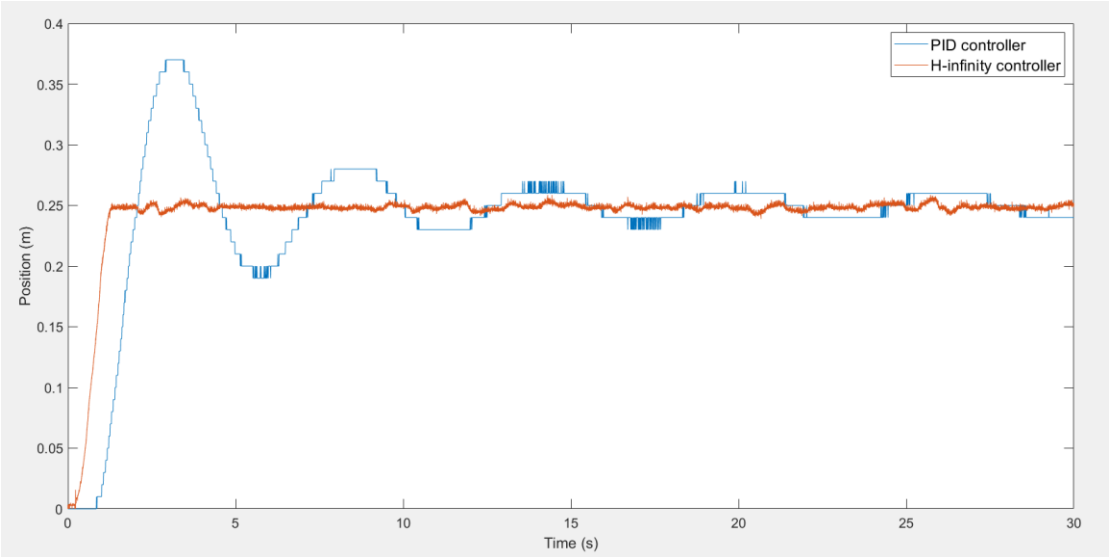

By adjusting supply pressure and additional load mass, the proposed H-infinity controller has almost the same characteristic, as shown in **Figure 4.18 – 4.19** while the PID controller behaves differently when faces with various conditions.

Figure 4.18

Position of the Cylinder Controlled by the Proposed H-infinity Controller at a Different Supply Pressure

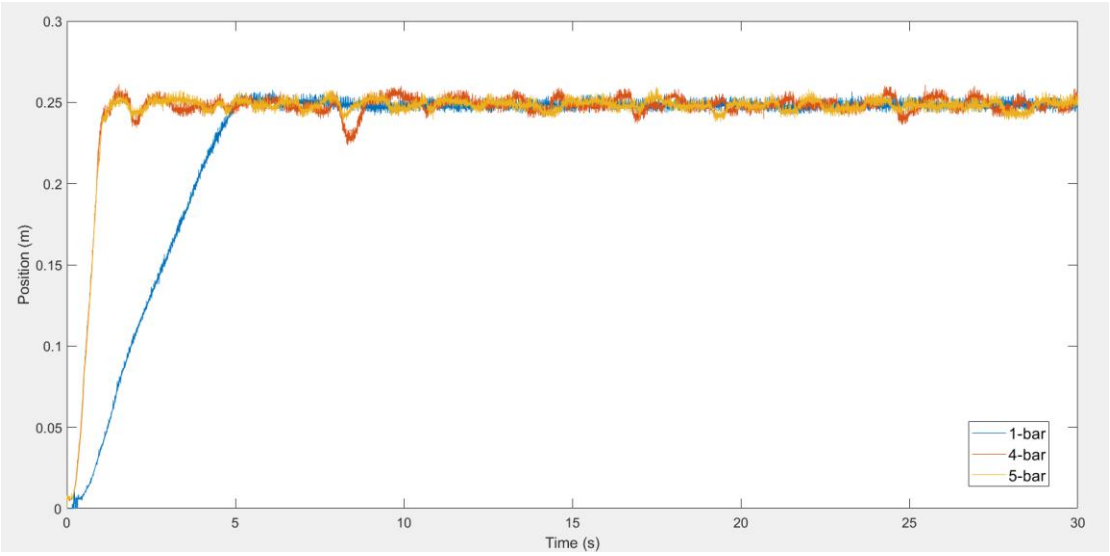

Figure 4.19

Position of the Cylinder Controlled by the Proposed H-infinity Controller with Different Additional Load Mass at a Nominal Pressure of 4 Bar (0.4 MPa)

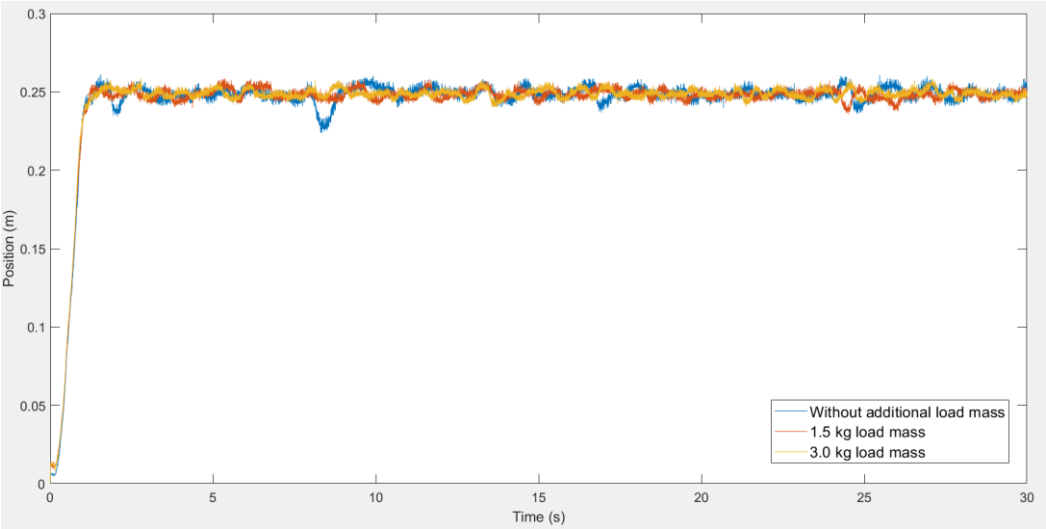

From **Figure 4.12** to **Figure 4.19**, the Root Mean Square Error (RMSE) and 100% Rise time could be determined to compare between the proposed H-infinity controller and the PID controller based on pole placement tuning method in table 4.1 and table 4.2 when they face uncertainties such as additional load mass and supply pressure. In addition, 0.0 kg refers to the system without additional load mass.

Table 4.1

H-Infinity Controller Analysis

	1 bar (0.1 MPa)			4 bars (0.4 MPa)			5 bars (0.5 MPa)		
Additional load mass (kg)	0.0	1.5	3.0	0.0	1.5	3.0	0.0	1.5	3.0
Root Mean Square Error (m)	0.0602	0.0636	0.0586	0.0325	0.0317	0.0314	0.0327	0.0322	0.0357
100% Rise time (s)	5.00	5.00	4.40	1.40	1.25	1.50	1.40	1.20	1.30

Table 4.2

PID Controller based on Pole Placement Tuning Analysis

	1 bar (0.1 MPa)			4 bars (0.4 MPa)			5 bars (0.5 MPa)		
Additional load mass (kg)	0.0	1.5	3.0	0.0	1.5	3.0	0.0	1.5	3.0
Root Mean Square Error (m)	0.1189	0.1150	0.0903	0.0265	0.0261	0.0233	0.0430	0.0419	0.04
100% Rise time (s)	9.15	9.50	9.30	2.60	2.23	2.28	2.05	2.09	2.06

According to the RMSE and 100% rise time, it can be seen that the RMSE of the PID controller at 4 bars where the plant model was identified is less than the RMSE of the proposed controller at every value of additional mass. However, the difference in the RMSE between these two controllers is only about 0.01 m. On the other hand, it is obvious that the 100% rise time or the time that the controllers take to bring the actuator to the setpoint for the first time of the proposed controller is smaller than the PID controller at any load mass. In addition, the lower the 100% rise time, the faster the actuator to the setpoint. Thus, the proposed controller could take the actuator to go to the setpoint faster than the PID controller with approximately 1.0 s at 4 bars (0.4 MPa) supply pressure.

Furthermore, the supply pressure is changed to investigate the robustness of the controllers. The RMSE of the H-infinity controller at both 1 bar (0.1 MPa) and 5 bars (0.5 MPa) is less than the PID controller at every value of the additional mass. The RMSE of the H-infinity controller is smaller than the PID controller just about 0.05 m and 0.001 m at 1 bar (0.1 MPa) and 5 bars (0.5 MPa), respectively. Moreover, the 100% rise time of the H-infinity controller is considerably smaller than the PID controller. The rise time difference between these two controllers is about 4.5 s at 1 bar (0.1 MPa). At 5 bars (0.5 MPa), the rise time of the proposed is less than the PID controller only 0.77 s which is almost the same as the one at 4 bars (0.4 MPa).

Moreover, the system with different setpoints for the cylinder has been introduced to the proposed controller, as shown in **Figure 4.20**. The setpoints are 0.15 m, 0.35 m, and 0.25 m. This experiment is used to shows that the proposed H-infinity controller is useable with a wide range of the position.

Figure 4.20

Position of the Cylinder at a Different Setpoint

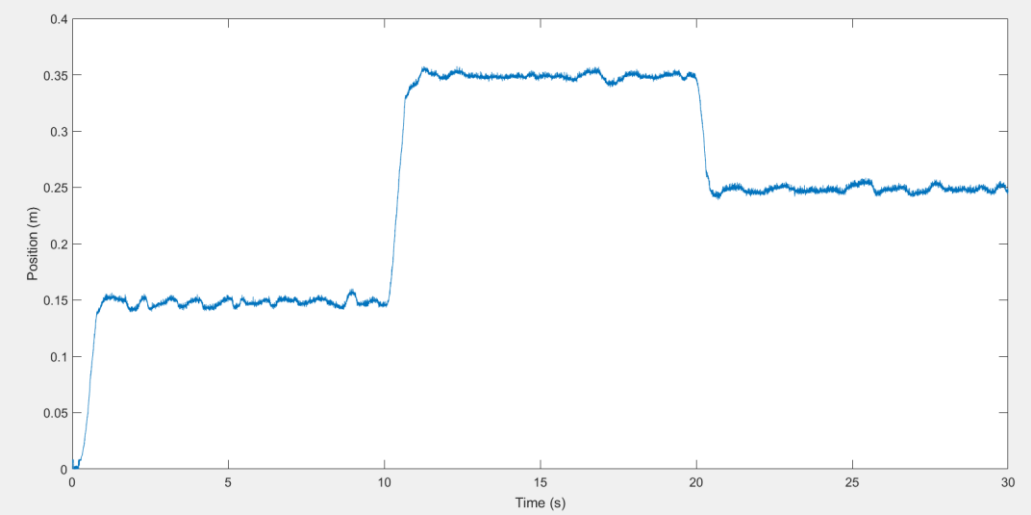

Furthermore, the 1.5 kg and 3.0 kg load mass are added to investigate the performance when the piston with additional mass has different desired locations, shown in **Figure 4.21** and **Figure 4.22**.

Figure 4.21

Position of the Cylinder at a Different Setpoint with 1.5 kg Load Mass

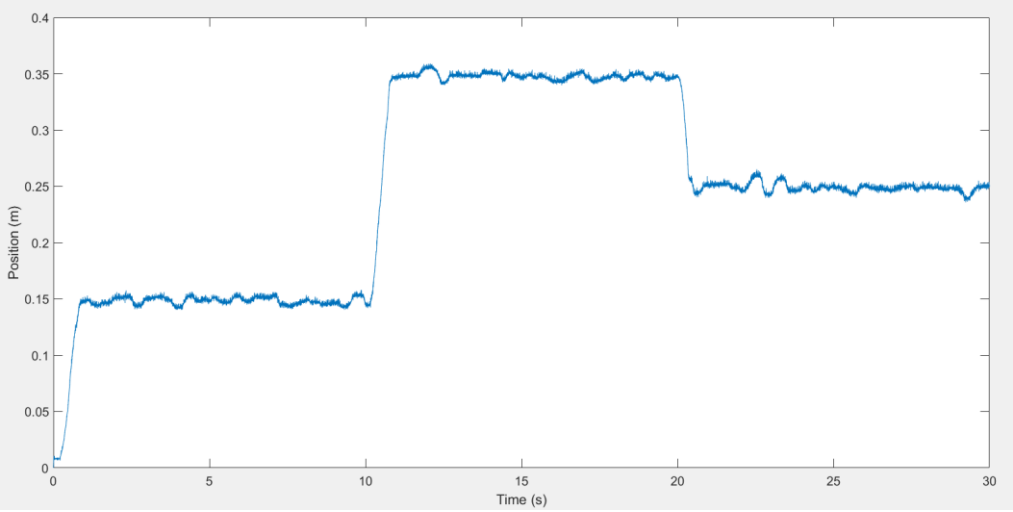

Figure 4.22

Position of the Cylinder at a Different Setpoint with 3.0 kg Load Mass

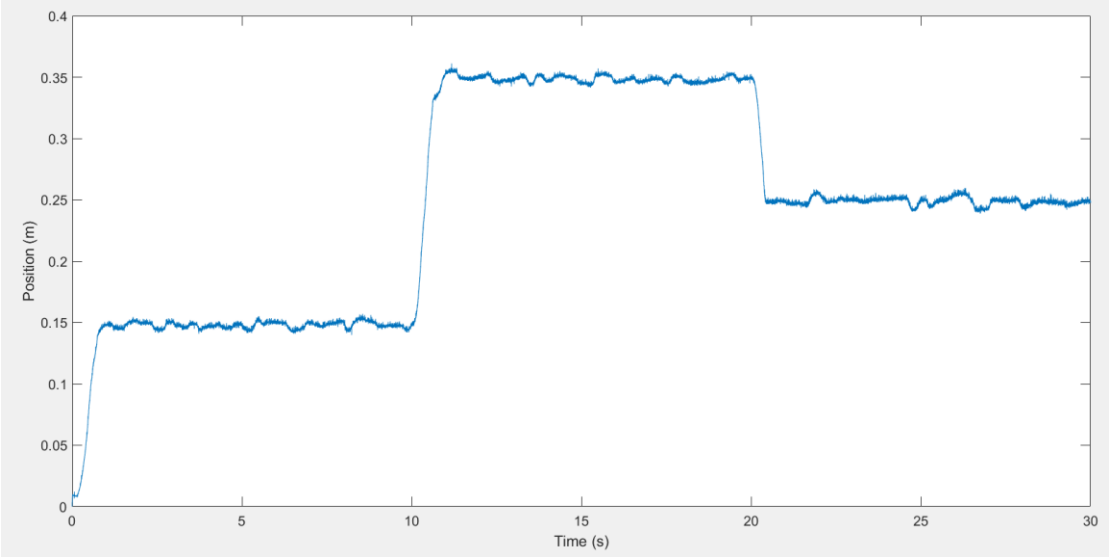

From **Figure 4.20** to **Figure 4.22**, the RMSE of the system is calculated to determine whether the proposed controller still well perform when faces a variety of additional load mass and different locations of the setpoint at 4 bars (0.4 MPa). The RMSE of the system without additional mass with different setpoints is 0.0251 m. Moreover, the RMSE of the system with 1.5 kg and 3.0 kg load mass is almost the same as the previous system. The values of the RMSE are 0.0253 and 0.0216 for 1.5 kg and 3.0 kg, consecutively.

CHAPTER 5
CONCLUSIONS AND RECOMMENDATION

5.1 Conclusion

The pneumatic system has experimented with two controllers which are a PID controller based on pole placement tuning method, and the proposed H-infinity controller to control the position of the pneumatic cylinder. The plant model is calculated at the nominal pressure of 4 bars (0.4 MPa) without any additional load mass. The proposed controller has been designed by a conventional H-infinity control. The controller is computed based on H-infinity optimal control synthesis via the γ-iteration method. The controller is designed as a full-order structure. By applying two weighting functions, the proposed controller successfully provides a good robust performance. The proposed controller has the optimal γ for which the cost function achieves under a preset limit of 0.9922. In addition, the gain and phase margin of the proposed controller is 2.26 dB, infinite deg, consecutively. The experiment result of the conventional H-infinity controller compares with the PID controller is done at various conditions. According to the measurement result of the position of the pneumatic piston, the RMSE and 100% rise time can be determined. It is shown that the cylinder controlled by the proposed one can go to the desired location faster than the PID controller in every condition. However, the PID controller provides a little bit better RMSE than the proposed controller at the nominal supply pressure. When the supply pressure is changed to 1 bar and 5 bars, it could be seen that the H-infinity controller can handle the change better than the PID controller according to the smaller RMSE. Furthermore, the additional load mass in the same level of the supply pressure could not affect the system much because the RMSE of the proposed controller is almost the same. Moreover, the overshoot of the cylinder controlled by the proposed controller is extremely less than the one controlled by the PID controller. Different desired locations of the cylinder also provide in order to verify the robustness of the designed controller. From the RMSE of the experiment with different desired locations, it could be told that several desired locations and additional load mass do not affect the performance of the proposed controller because it still provides the RMSE close to the system with only one desired setpoint.

To summarize, this paper designs a full-order H-infinity optimal controller. Although, the structure of the controller is complex, the designed controller guarantee that it can be used with a nonlinear system such as the pneumatic system as shown in this paper.

5.2 Recommendation

1. Design the H-infinity controller with other weighting functions. Because the weighting function used in this study comes from a method like trial-and-error, it might have another value of weighting function that provides a better result.
2. Estimate the plant with higher order than the second-order because it could describe the characteristic of the pneumatic system better than the one in this work.
3. Due to the modification of the generated voltage by op-amp provided by the microcontroller is not accurate and different from the calculation, the position of the cylinder has some error. More precise voltage modification is required to provide a better result of the cylinder's position.

REFERENCES

M. Karpenko, N. Sepehri (2004, June 30 – July 2). *Design and experimental evaluation of a nonlinear position controller for a pneumatic actuator with friction*. Proceedings of the 2004 American Control Conference, Boston, MA, USA.

J. Wang, J. Pu, P. Moore (1999). A practical control strategy for servo-pneumatic actuator systems. *Control Engineering Practice, 7(12),* 1483-1488.

P. Korondi, J. Gyeviki (2006, August 30 – September 1). *Robust Position Control for a Pneumatic Cylinder*. 2006 12th International Power Electronics and Motion Control Conference, Portoroz, Slovenia.

J. Song, Y. Ishida (1997). A robust sliding mode control for pneumatic servo systems. *International Journal of Engineering Science, 35(8),* 711-723.

J. Doyle, K. Glover, P. Khargonekar, B. Francis (1988, June 15-17). *State-space solutions to standard H_2 and H_∞ control problems*. 1988 American Control Conference, Atlanta, GA, USA.

F. Meng, A. Pang, X. Dong, C. Han, X. Sha (2018). H_∞ Optimal Performance Design of an Unstable Plant under Bode Integral Constraint. *Complexity, 2018,* 10. https://doi.org/10.1155/2018/4942906

W. Tuvayanond, M. Parnichkun (2017). Position control of a pneumatic surgical robot using PSO based 2-DOF H_∞ loop shaping structured controller. *Mechatronics, 43,* 40-55.

R. Kaur, J. Ohri (2014). H-infinity controller design for pneumatic servosystem: a comparative study. *International Journal of Automation and Control, 8(3),* 242-259.

S. Kaitwanidvilai, M. Parnichkun (2004). Genetic-Algorithm-Based Fixed-Structure Robust H Loop-Shaping Control of a Pneumatic Servosystem. *Journal of robotics and mechatronics, 16,* 362-373.

S. S Nair (2011). Automatic weight selection algorithm for designing H infinity controller for active magnetic bearing. *International Journal of Engineering Science and Technology, 3(1),* 122-138.

RW. Beaven, MT. Wright, DR. Seaward (1996). Weighting function selection in the H_∞ design process. *Control Engineering Practice, 4(5)*, 625-633.

I. El-Sharif, F. Hareb, A. Zerek (2014). Design of discrete-time PID controller. *International Conference on Control, Engineering & Information Technology (CEIT'14)*, 110-115.

W. Backe, and O. Ohligschlaeger (1989). Model of heat transfer in pneumatic chambers. *Journal of Fluid Control, 20(1)*, 61-78.

L. Ljung (1999). System Identification: Theory for the User. *Prentice Hall 2nd edition*.

K. Hamiti, A. Voda-Besancon, H. Roux-Buisson (August 1996). Position control of a pneumatic actuator under the influence of stiction. *Control Engineering Practice, 4(8)*, 1079-1088.

M. Shih, S. Tseng (1995). Identification and position control of a servo pneumatic cylinder. *Control Engineering Practice, 3(9)*, 1285-1290.

M. Uebing, and N. D. Maughan (1997). On linear modeling of a pneumatic servo system. *Proceeding of the Fifth Scandinavian International Conference on Fluid Power, 2*, 363-378.

H. Garnier, M. Mensler, and A. Richard (2003). Continuous-Time Model Identification from Sampled Data: Implementation Issues and Performance Evaluation. *International Journal of Control, 76(13)*, 1337–1357.

L. Ljung (2009). Experiments with Identification of Continuous Time Models. *IFAC Proceedings 42(10)*, 1175–80.

K. Zhou, and J. Doyle (1998). Essential of Robust Control. *Prentice Hall*.

G. Zames (1981). Feedback and optimal sensitivity: Model reference transformations, multiplicative seminorms, and approximate inverses. *IEEE Transactions on Automatic Control, 26(2)*, 301–320.

JW. Helton (1978). Orbit structure of the Mobius transformation semigroup action on H-infinity (broadband matching). *Adv. Math. Suppl. Stud. 3*, 129–197.

A. Tannenbaum (1980). Feedback stabilization of linear dynamical plants with uncertainty in the gain factor. *International Journal of Control, 32(1)*, 1–16. https://doi.org/10.1080/00207178008922838